53

NASA TN D-1267

TECHNICAL NOTE

D-1267

CURRENT ESTIMATES OF RADIATION DOSES IN SPACE

By Trutz Foelsche

Langley Research Center
Langley Station, Hampton, Va.

NATIONAL AERONAUTICS AND SPACE ADMINISTRATION
WASHINGTON
July 1962

TABLE OF CONTENTS

NATIONAL AERONAUTICS AND SPACE ADMINISTRATION

TECHNICAL NOTE D-1267

CURRENT ESTIMATES OF RADIATION DOSES IN SPACE[1]

By Trutz Foelsche

SUMMARY

A gross survey of data on energetic radiation in the environment of the earth is presented. This survey embraces the Van Allen belt radiations, galactic cosmic radiations, and solar cosmic radiations associated with solar flares. In the light of the current data the radiation problem is analyzed in terms of shielding requirements to keep exposure down to "tolerable" limits in manned space flights. The estimates are preliminary, especially in the cases of chance encounter with flare protons, since the available data are incomplete and only allow calculations of upper and lower limits of physical doses. Also the contribution of certain primaries and secondaries to the biological effect is not finally known.

INTRODUCTION

There are known today three kinds of energetic radiations existing in interplanetary space, which constitute a potential radiation hazard for manned space flight:

(1) The Van Allen belt radiations: energetic particles of substantial intensity trapped in the magnetic field of the earth and probably in the magnetic field of planets.

(2) Galactic cosmic radiation: protons and heavier ions arriving from all directions of the galaxy, in part having extreme energies but of low intensity. This intensity in free space, of course, is substantially higher than that of their secondaries at sea level on earth, where man is protected by an atmospheric shield equivalent to 10 meters of water and in medium and low latitudes by the magnetic field of the earth, which deflects these particles.

(3) Solar cosmic radiation: identified during the International Geophysical Year as transient energetic proton showers associated with

---

[1]This report was presented in abbreviated form as Paper No. CP 61-1143 entitled "Radiation Hazards in Space" before the American Institute of Electrical Engineers, Fall General Meeting (Detroit, Mich.), Oct. 15-20, 1961.

flares on the sun. Flares are intense chromospheric light flashes in the visible and ultraviolet part of the spectrum accompanying violent plasma eruptions on the sun's surface. In some cases the proton streams encountering the earth have high intensity and a duration in the order of days.

The purpose of this survey is to describe hazards produced in space vehicles by these radiations in an approximate and gross way by giving dose rates and doses in the center of spherical shields of various wall thicknesses. The doses produced by belt and flare radiations that are most important with respect to acute radiation hazards are reviewed in more detail. Dose rate calculations for Van Allen Belt protons, based on Freden-White's spectrum and neglecting nuclear collisions, were carried out by Hermann Schaefer as early as 1959 (see refs. 1 to 3). For 1960 proton dose rate calculations taking into consideration nuclear collisions and secondaries and also X-ray dose rate calculations were presented by Keller and Schaeffer and by Allen, Dessler, Perkins, and Price (see refs. 4 and 5)[2]. By the same authors, dose rate and, in part, dose calculations also have been made for the May 1959 solar proton event based on the spectrum and data given by Winckler. (See ref. 6.) Upper and lower limits of doses including those for the July 1959 low-energy and February 1956 high-energy events were treated by the present author in January 1961 (ref. 7), based mainly on spectra of Winckler and Bailey (refs. 8 and 9). In the present paper, in addition, upper limits of spectra at 3 different instants for the November 12, 1960 solar proton event are estimated (fig. 9) on the basis of the data and spectra given by Van Allen, Winckler, Ney, Fichtel and Guss, and by Davis and Ogilvie, and on the neutron intensities measured in Deep River, Canada, by Steljes, Carmichael, and McCracken. Since for this event data are available during a great part of the time of significant proton influx, the time-integrated fluxes resulting from these spectra and the calculated time-integrated dose rates or total doses are more certain than in other treated events. The large amount of data obtained for the November 1960 events is of great value for dose estimates, since these events were extreme in intensity and duration and since further events of this magnitude are improbable before 1967.

In the calculations on flare protons, mainly electronic collisions of the primaries in the shield are assumed. The result of the calculation is expressed in physical doses (rep or rad). A summary of the radiation levels of galactic cosmic radiation, belt radiations, and solar cosmic radiations as obtained from the various estimates is presented in table I. The contribution of secondaries originating in nuclear collisions to the physical flare proton doses has recently been estimated by scientists of Lockheed Nuclear Products. The physical doses do not fully determine the

---

[2]These calculations are cited by the author because of their early availability and this selection does not imply judgment of work of authors not cited.

biological effect. Also in the case of galactic cosmic and belt radiation for a more exact appraisal of the biological effects, the contribution of secondaries produced in nuclear collisions within the vehicle, the shielding, and the human body, and the different biological effects of the various physical doses throughout the body have to be investigated further and taken into account. Also included must be the shielding effect of the body itself. The given dose rates and doses are thus only rough approaches with emphasis on upper limits, which are approximately valid for shielding up to 15 to 20 g/cm^2, rather than a detailed and final assessment of the biological effects on men behind high shielding thicknesses and in large space vehicles. The used radiobiological units and terms, and physical symbols are defined in the appendix. The formerly used unit rep = 93 erg/g absorbed energy for the physical dose, retained in this report in some figures and the corresponding text for reasons of correctness can be replaced in any case by rad = 100 erg/g without significantly affecting the results. The implicit enhancement of 7 percent in the dose values is considered as insignificant in the light of present uncertainties. In the appendix, furthermore, the basic data and methods used for flare proton dose calculations are given in detail.

VAN ALLEN BELT RADIATIONS

Spatial Distribution, Energies and Fluxes of Trapped Particles

Figure 1 presents a survey of the spatial distribution and the intensities of the energetic belt particles. In the upper part of figure 1 the isocount lines are drawn by Van Allen according to counter measurements (refs. 1, 10, and 11) with satellites Explorer I, Explorer IV, and in the outer region with Pioneer IV, March 3, 1959, after a major solar activity period. The results indicate two regions of maximum intensity, one at 10,000 kilometers from the earth's center and one at a more distant region of about 25,000 kilometers.

In the lower part of figure 1 are shown isocount contours and measurements with ionization chamber in Explorer VI at quiet times (August 1-16, 1959) of Winckler and coworkers. (See ref. 12.) At this time the outer region is considerably shrunken and shows two maxima of intensity. During magnetic storms following this quiet period, further depletion of the outermost zone was observed. This depletion was, in turn, followed by a large increase in the intensity and expansion of the outer belt. The intermediate belt disappeared and similar count contours were obtained such as those in the upper part of figure 1. A more quantitative comparison of the variation of intensities in the outer zone can

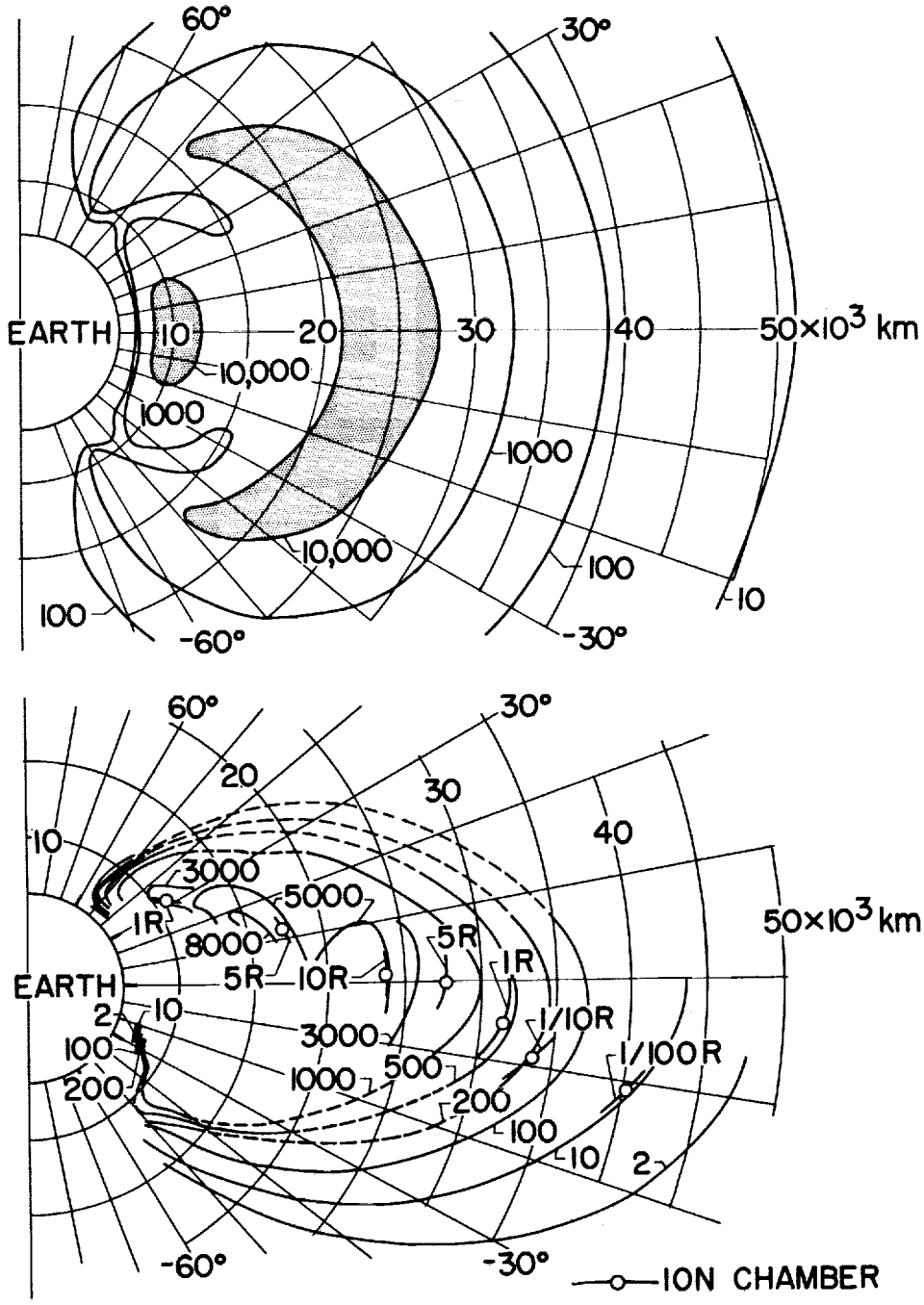

Figure 1.- Comparison of the counting rate contours in the radiation zone as given by Van Allen (upper) and as given by analysis of Explorer VI (lower) shown on a polar plot. It is apparent that the radiation zones during the time of Explorer VI have shrunken considerably and changed form since those inferred from the Explorer IV and Pioneer III and IV data. (Figures taken from ref. 12.) R denotes rad per hour.

be obtained from figure 2 (ref. 12), which shows the counts in lightly shielded counters during flights radial outwards. Pioneers III and IV had almost identical Geiger Mueller counters (shielding of about 1 g/cm^2 of the same material) and nearly identical trajectories. More recent measurements revealed that the count contours in figures 1 and 2 in the outer regions reflect mainly the intensities of high-energy electrons ($E > 2.5$ Mev) of low flux and their strong intensity variations with time during solar disturbances of the geomagnetic field. The bulk of trapped particles appears more stable, especially in the inner zone. Particles, energies, and flux distributions that are observed are about as follows:

(1) High-energy protons (30 Mev < E < 700 Mev). They are only found within the inner belt and its near environment (slot) and have an integral intensity in the center, according to measurements with Pioneer III, in the order of 2×10^4 particles/cm^2-sec ($E > 40$ Mev). The intensity of these high-energy protons appears to vary, especially in the low-energy part of the spectrum observed down to at least 8 Mev (ref. 13), slowly and not in a uniform manner by a factor of 2 to 3 in correlation with flare activity on the sun, as observed from October 1959 to December 1960 with Explorer VII (ref. 14).

(2) Low-energy protons (120 kev < E < 4.5 Mev) having orders of magnitude higher intensities. They are observed to extend from a radial distance of 2.5 earth radii up to 8 to 10 earth radii throughout the entire outer zone. A flat intensity maximum ($\dot{N} = 10^8$ to 10^9 protons/cm^2-sec, $E > 120$ kev) extends symmetrically to the magnetic equator plane in a radial distance of about 3 to 5 earth radii. These measurements were reported at a Symposium on Explorer XII, January 1962, by L. R. Davis and J. M. Williamson of the NASA Goddard Space Flight Center.

(3) Low- and medium-energy electrons (45 kev < E < 1.6 Mev) with high intensity ($\dot{N}_{max} \approx 10^8/cm^2$-sec, 45 kev < E < 1.6 Mev, ref. 15; $\dot{N}_{max} \approx 5 \times 10^8/cm^2$-sec ster, $E > 10$ kev, Davis and Williamson). They constitute the second main component, which extends through both belt regions. Their integral intensity seems to vary in a lower degree with magnetic disturbances and remains high (10^5 to $10^6/cm^2$-sec ster) near the earth right up to the auroral zone ($\lambda_{magn} = 67.5^\circ$ N) and toward the distant edge of the outer belt according to measurements with Explorer XII (ref. 15 and measurements of Davis and Williamson). The intensity of electrons and their upper limit of energy within the inner belt especially in the center seems uncertain at present. Preliminary estimates of fluxes in the heart of the inner belt are:

$\dot{N} < 2 \times 10^7/cm^2$-sec ster, $E > 600$ kev, 3,600-km altitude
(Van Allen and coauthors, ref. 14)

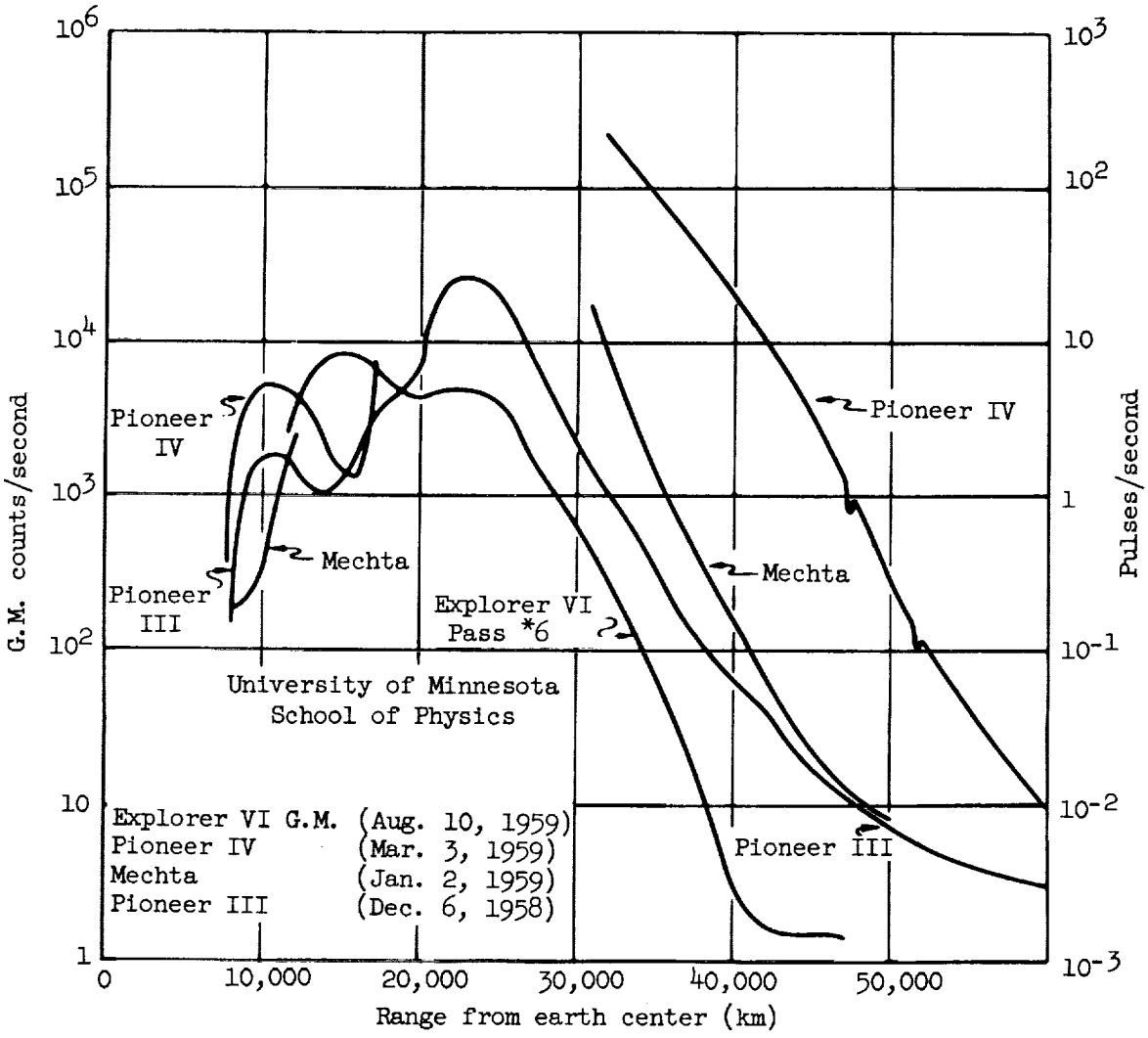

Figure 2.- Comparison of Geiger Mueller counter rates for Explorer VI, Pioneer III, Pioneer IV, and the Russian Mechta space probe. The various counting rates are on a comparable basis within approximately 25 percent. Explorer VI shows the lowest intensity of trapped radiation and Pioneer IV the greatest enhancement of the radiation regions. These curves illustrate the time variability of the outer regions over long periods. (Figures taken from ref. 12.)

$\dot{N} \approx 1 \times 10^7/cm^2\text{-sec}$, $E > 500$ kev
$\dot{N} \approx 2 \times 10^9/cm^2\text{-sec}$, $E = 200 - 500$ kev
} (Hoffman, Arnoldy, and Winckler, ref. 16)

In lower altitudes are observed intensities of electrons

$E > 40$ kev of $2 \times 10^6/cm^2\text{-sec ster}$ { (Injun I, 1,000-km altitude, ref. 14)

and

$E > 600$ kev of $4.5 \times 10^5/cm^2\text{-sec ster}$
and $3 \times 10^5/cm^2\text{-sec ster}$
} (Explorer IV, ref. 14)

The latter at invariant radius $r = 1.25$ and in magnetic shells $L = 1.3 - 2.2$ (slot), respectively. (Definitions of r invariant and L are given in ref. 14.)

(4) Superimposed to these "low"-energy electrons are, in the outer zone, high-energy electrons $E > 1.6$ Mev of lower flux (maximum flux, 10^5 to $10^6/cm^2$-sec, $E > 1.6$ Mev; see also Vernov et al., refs. 17 and 18; $<10^3/cm^2$-sec, $E > 5$ Mev, peaked at about 20,000- to 25,000-km radial distance) that exhibit strong variations in intensity (factor 50 to 100) at the peak and toward greater distances.

Proton Dose Rates (Inner Belt)

To calculate the dose rates behind various amounts of shielding arising, for instance, from protons in the center of the inner belt, it is necessary to know the energy spectrum of the particles.

The spectrum of protons above 75 Mev in the inner belt was first measured with nuclear emulsions by Freden and White (ref. 2), but only near the lower belt boundary at an altitude of 1,200 kilometers near Cape Canaveral, 80° W., in magnetic latitudes between 20° and 30° N. (7 April 1959). The flux was extrapolated down to 40 Mev and estimated as 1,000 protons/cm^2-sec. The proton spectra on different locations of the inner zone measured in more recent times[3] fall off with energy more

---

[3]For example, Sept. 19, 1960, rocket from NASA Wallops Station, $\lambda_{magn} \approx 30°$ N., <1,900-km altitude (ref. 13); Aug. 1959, Explorer VI, Indian Ocean, Australia, $\lambda_{magn} \approx 27°$ S., <2,500-km altitude (ref. 16); October 13, 1960, Atlas, Middle Atlantic, $20° < \lambda_{magn} < 30°$ N., <1,185-km altitude (ref. 19); July and October 1961, Midas III and IV polar satellites, respectively, λ_{magn} from 0° to 30°, 3,450 and 3,510 to 3,760-km altitude, respectively (ref. 20).

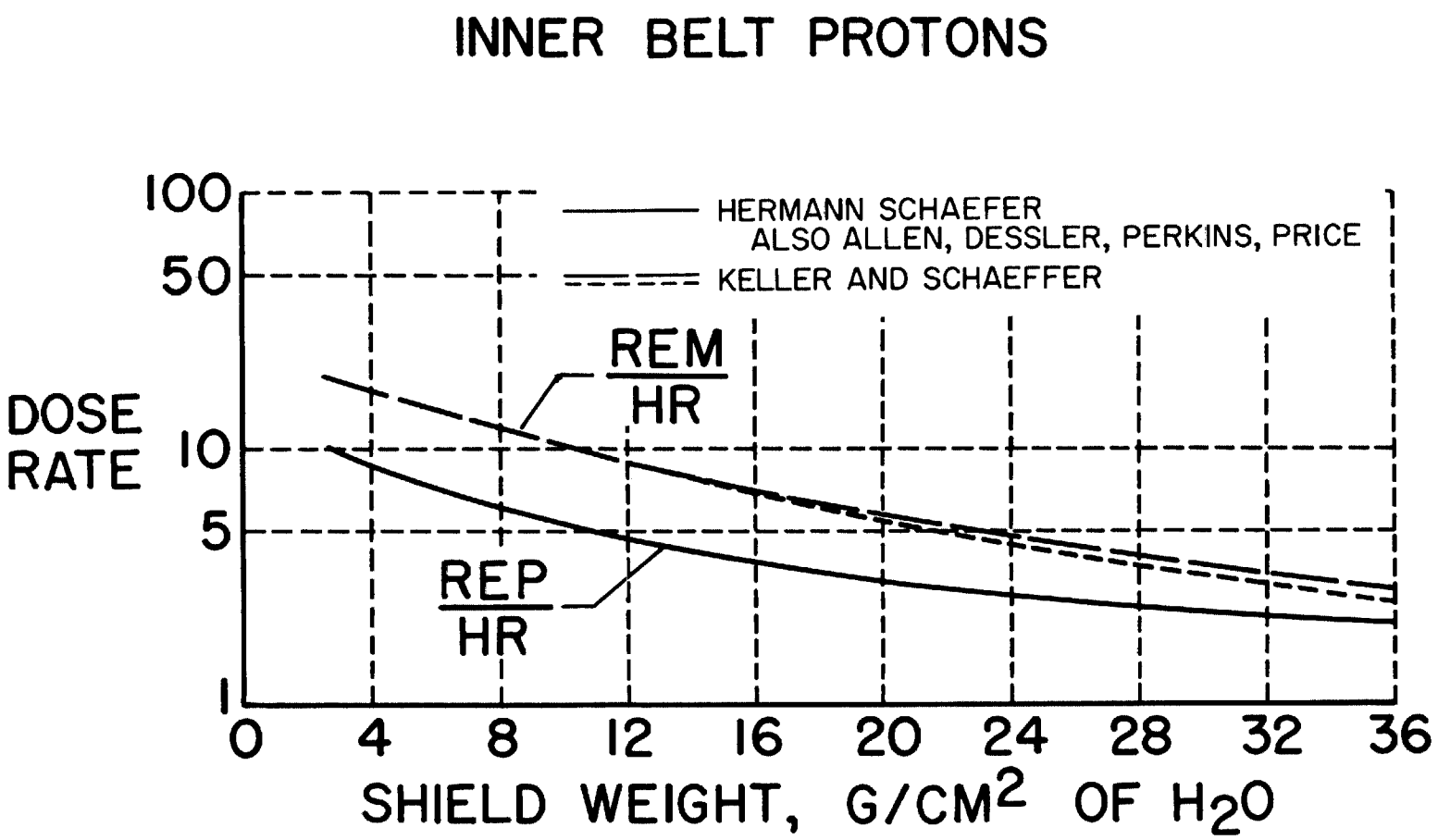

Figure 3.- Dose rates in center of spherical shields neglecting self-shielding of the body. The rem dose rates are calculated (ref. 4) by assuming for protons and neutrons of $E > 40$ Mev RBE = 1 and of $E < 40$ Mev RBE = 2. The long-dashed line indicates the contribution of neutrons. This contribution would be higher by a factor of about 5 (based on the calculations in ref. 21) by assuming RBE $\approx$ 10 for neutrons $E > 1$ Mev.

steeply than or about equally as the Freden-White spectrum. This means that the penetration power of the protons at specific locations, especially in the center of the belt, is lower than calculated on the basis of the Freden-White spectrum. To arrive at upper limits of doses inside larger shield thicknesses, the calculations based on the Freden-White spectrum may be cited (refs. 3 to 5). By normalizing this spectrum to 20,000 protons/cm^2-sec of energies $E > 40$ Mev in the center, the results are essentially the same and are shown in figure 3.

H. Schaefer[4] and Allen and coauthors came to essentially the same dose rate in rep/hour behind different amounts of shielding (lowest curve of fig. 3). The higher values of Keller and Schaeffer in rem/hour are partly caused by the assumption that protons and neutrons of energies <40 Mev have an RBE = 2 and partly by a somewhat different extrapolation of the low-energy part of the spectrum. Under the assumption that the spectrum has the same shape in the center of the inner belt as at the inner edge, self-shielding being neglected and a maximum value of 20,000 protons/cm^2-sec with energies of >40 Mev being assumed, there are obtained inside a spherical water shield the following dose rates:

Wall thickness, g/cm^2 of H_2O	Dose rate, rep/hr
2	12
25	2.7

The dose rate decreases only by a factor 1/4 to 1/5 by using a heavier shield of 25 g/cm^2 of H_2O or carbon.

In order to provide for possible error in the maximum intensity of protons and also for variations in the intensity that have been recently reported, an average flux of 40,000 protons/cm^2-sec ($E > 40$ Mev), and the number of 24 rep/hr behind shielding of 2 g/cm^2 appears preferable as the average proton dose rate in the center of the inner belt and correspondingly approximately 6 rep/hr behind shielding of 25 g/cm^2.

---

[4]The lowest curve in figure 3 is deduced from H. Schaefer's "Bragg" curve for a parallel beam with Freden-White's energy spectrum by multiplying by the factor 20 $\left(\text{that is, } \frac{20{,}000 \text{ protons/cm}^2\text{-sec (center)}}{1{,}000 \text{ protons/cm}^2\text{-sec (1,200 km)}}\right)$, self-shielding of the body not being considered. Schaefer calculated also the self-shielding effect behind different amounts of outer shielding based on this "Bragg" curve for the spectrum considered and the depth dose-rate distribution in a spherical body phantom for belt and flare proton spectra.

Estimates taking into account secondaries from nuclear collisions, especially fast neutrons, are carried out in references 4 and 5 for different structure and shielding materials like Be, C, Mg, and Al, with the result that the contribution to the physical dose rate for shielding thicknesses of the order of 20 g/cm^2 is about 10 percent in first approximation. It seems advisable to refine these calculations by taking into account also the contribution of neutrons and γ-rays produced by low-energy protons ($\approx$20 Mev) which may be high (for example for Be) and to estimate the biological dose rate in more detail. On the basis of an RBE factor of 5 to 10 for neutrons in the Mev energy range values which appear justified by experience for neutrons from 0.5 to 10 Mev, the theoretical approaches indicate that inside walls with greater thicknesses such as those of aluminum, secondary neutron radiation contributes substantially to the biological dose in rem. There still exist uncertainties in the rem dose values for large shield thicknesses, partly because, for different materials, the spectra of the penetrating secondaries are not exactly known and partly because the RBE factors of neutrons of different energies and of nuclear collisions in the human body are not well known.

X-Radiation Inside the Vehicle

As the second factor contributing to the radiation exposure of the crew within the belts, X-radiation inside the compartment produced by electrons impinging on the surface of the spacecraft must be considered. Within the belts electrons having energies between 40 Kev and 2 Mev or even more - in the low-energy range of high intensity - are measured. Electrons of 100 Kev have only a practical range less than 30 mg/cm^2 in aluminum; electrons of 2 Mev have approximately 1 g/cm^2 practical range. Since the wall of the spacecraft has in any case at least some g/cm^2 thickness, electrons in the range of 1 to 5 Mev will not have immediate effects. In quiet periods, Winckler (ref. 8) measured directly 10 rad/hr with an ionization chamber of 1/2 mm or 135 mg/cm^2 aluminum wall thickness. In the expansion phase after magnetic storms, the dose rate increased to 30 rad/hr in Explorer VI. These ionization rates are in part the result of X-radiation produced in the wall and in part the result of penetrating electrons themselves.

Although the electron fluxes are high (the electron flux $E > 20$ Kev is estimated to be larger than 10^8 electrons/cm^2-sec at the peak of the inner and outer belt), the problem of shielding against the produced X-radiation is of lower magnitude than that of shielding against the energetic protons in the inner belt. The intensity of all X-radiation having energy less than 100 Kev is strongly attenuated by a few millimeter of steel or other high Z-number material used as construction material of spacecraft (2-mm steel attenuates a dose rate of 100 r/hr, if the X-radiation has energies <100 Kev, by more than a factor 100 to 1 r/hr). An outer coat of carbon or even hydrocarbon ablation material instead of aluminum would reduce the produced X-ray intensity further by a factor

of 3, since the produced X-ray intensity is proportional to the Z-number. The results of more detailed calculations depend strongly on the assumed electron spectra and on constructive details such as wall materials and thicknesses. With spectra given by Van Allen (ref. 10), Holly and Johnson (ref. 22), and Walt et al. (ref. 23), detailed calculations for different materials were carried out in references 4, 5, 24, and 25 as well as by staffs of other laboratories. As an example for an upper limit of X-ray dose rate inside conventional wall materials, the result of Robley Evans (ref. 25) may be cited. As material of the outer shell 30-mil (0.6 g/cm^2) steel was assumed. By using as a basis the flat electron spectrum measured by Walt et al. on the inner leg of the outer belt at 1,000-km altitude, magnetic latitude 45° north (near Wallops Island, Va.), and assuming a total flux of 10^{11} electrons/cm^2-sec of $E > 20$ Kev in the center of the outer belt, Evans obtained a dose rate of 2 rad/hr. A. J. Dessler (ref. 5) concluded from energy flux measurements of Vernov et al. (refs. 17 and 18) and the spectrometer results of Walt et al. (ref. 23) that the electron flux ($E > 80$ Kev) should be in the order of only 10^8 electrons/cm^2-sec. This value was reaffirmed by O'Brien, Van Allen, and coworkers on the basis of Explorer XII data measured with unambiguous detectors (ref. 15). According to these measurements, the intensities are in the following limits:

E	Intensities, electrons/cm^2-sec
45 to 60 Kev	$9\ ^{+\ 16 \times 10^7}_{-\ 6 \times 10^7}$
80 to 110 Kev	$8\ ^{+\ 16 \times 10^7}_{-\ 5 \times 10^7}$
110 Kev to 1.6 Mev	$<10^8$
1.6 Mev to 5 Mev	$2 \pm 1 \times 10^5$
>5 Mev	$<10^3$

Although higher energy electrons are observed (Walt et al. measured the spectrum only up to 400 Mev), the safety factor in this spectrum $\approx 10^{10}$ electrons/cm^2-sec of $E > 200$ Kev) is so high that the given value of 2 rad/hr appears nevertheless highly conservative especially for a typical spacecraft with carbon-covered steel and aluminum walls of some g/cm^2 thickness.

If these maximum dose rates - the proton dose rate of 6 to 24 rep/hr in the inner belt dependent on shielding and of some rem/hour X-radiation in the outer belt - are compared with the doses characteristic for radiation sickness (that is, 100 to 200 rem), it can be recognized that for a trip straight through the belts, that is, passing the inner belt in about 10 minutes and the outer belt in about 2 hours, no acute radiation symptoms should be anticipated.

The radiation hazard increases very rapidly if the spacecraft stays within the inner belt, for instance, for longer periods. Even with heavy

shielding of 25 g/cm^2, the crew would receive in 24 hours more than 150 rem in the center of the inner belt.

The high doses produced by the electrons and also low-energy protons (0.1 to 5 Mev) directly on the surface of the vehicle may be furthermore mentioned. By assuming fluxes $>10^8$ to 10^9 particles/cm^2-sec of protons and electrons in the outer belt, dose rates of 0.5 to 1×10^6 rad/hr are obtained; these dose rates have damaging effects on, for example, unprotected photovoltaic cells and possibly even on plastics used in communication satellites, if they remain for months and years inside the belt regions. For extended periods also the penetrating belt radiations should constitute a limiting factor for the use of certain electronic devices (e.g., transistors) inside the vehicle.

GALACTIC COSMIC RADIATION

Intensities and Overall Ionization Dosage

The primary galactic cosmic radiation consists of positively charged atomic nuclei of high energy, mostly protons ($\approx$85 percent), α particles ($\approx$13 percent), and a few heavier nuclei observed up to tin (Sn), stripped of all electrons. Figure 4 gives an illustration of the cosmic-ray intensities near the earth and their variation with solar activity. It shows a meridional cross section of the overall ionization on top of the atmosphere (for about 10 g/cm^2 atmospheric depth, that is, 100,000-ft or 30-km altitude) produced by galactic cosmic rays and their secondaries. During solar minimum years, the ionization is higher by a factor of about 2 above the poles. As is shown near the origin of the abscissa, the ionization above the magnetic equator at an altitude of 30 km is low as a result of the shielding effect of the magnetic field of the earth and is about equal during solar maximum and solar minimum years. The increase of ionization during solar minimum years by a factor of about two on the poles and not on the equator reflects the fact that the low-energy part of the primary spectrum is increased during this period, since only the low-energy particles have access to the poles but not to the magnetic equator. This fact is of certain biological significance, which is discussed subsequently. (See section on "Heavy Primary Hits.")

During solar activity years sudden further decreases of ionization of as much as 25 to 30 percent are observed. These so-called "Forbush decreases" are associated with solar-flare activity. Simultaneous observations (ref. 26) of such decreases both on earth and aboard space probe Pioneer V (1960 Alpha) during 1960 and at 5,000,000 kilometers from the earth indicate that they are due not to distortion of the earth's magnetic field but to interplanetary magnetic clouds associated with ejected solar plasmas.

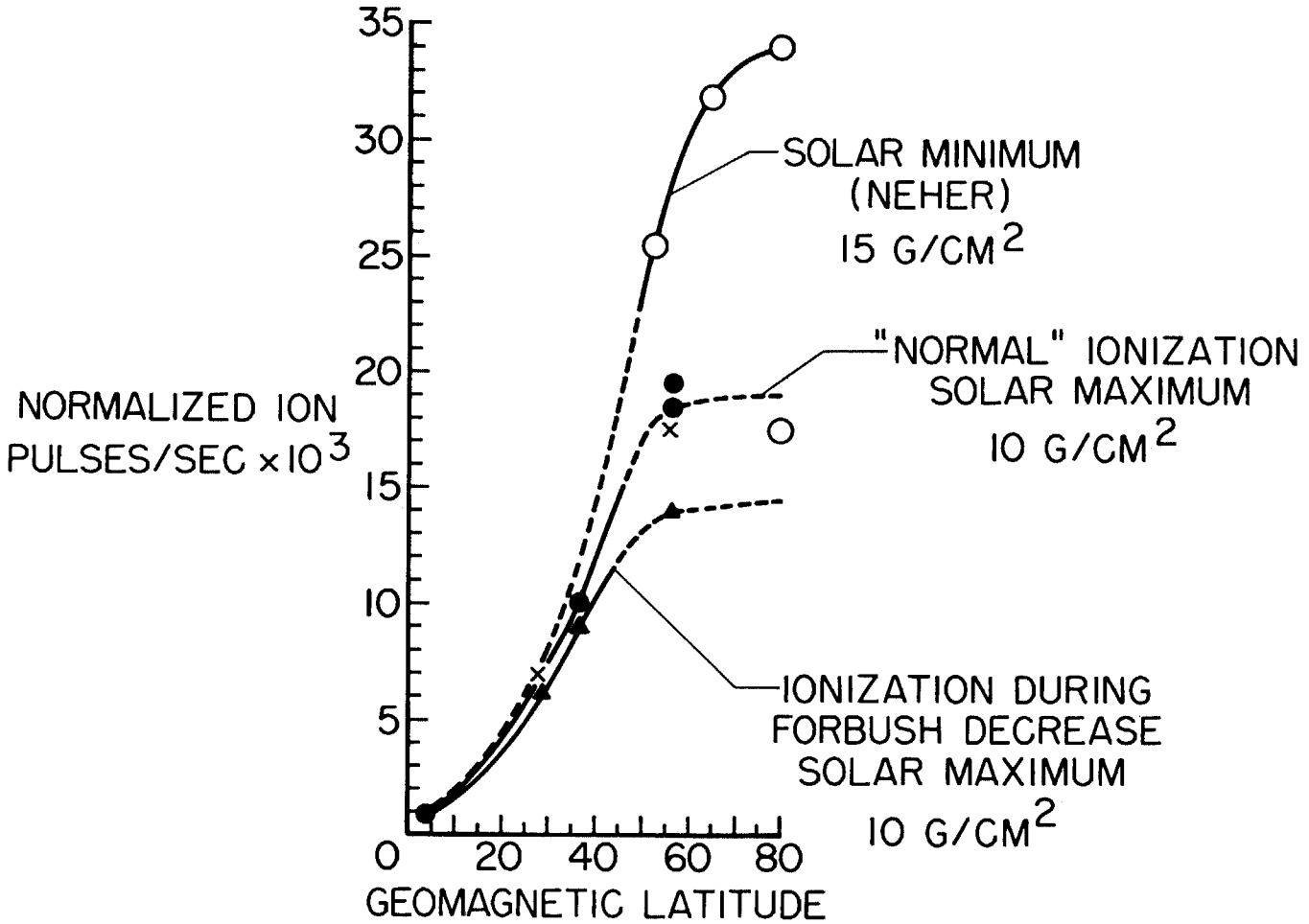

Figure 4.- Total ionization in 10 g/cm^2 depth of atmosphere as a function of geomagnetic latitude at solar minimum and maximum. (Reproduced from ref. 6, J. R. Winckler.)

From the general viewpoint of implications to space flights, the most important fact is that the flux of galactic cosmic rays in interplanetary space is very low in comparison with the flux in the belt or in major solar proton beams, namely,

$$N = 2.5 \frac{\text{particles}}{\text{cm}^2\text{-sec}}$$

during solar activity years. This flux is about four orders of magnitude lower than the maximum flux in the inner belt. It may be supposed, therefore, that the normal ionization dosage of galactic cosmic rays lies under any acute level. By carefully taking into account the higher specific ionization of heavier primaries and their higher RBE, a dose rate of about 0.45 rem/week in free space is calculated, if no shielding is provided, except self-shielding of the body (refs. 27 and 28) and secondaries produced in the body are neglected. The maximum permissible dose rate for radiation workers is at present 0.1 rem/week or 5 rem/year for persons from ages 18 to 68 or a total of 250 rem during an adult's lifetime (ref. 29). Thus, the normal ionization dosage by galactic rays should at least not lead to acute or disabling symptoms, even if the spacecraft crew is exposed to this space radiation for a year or more (25 to 50 rem), and even if secondaries produced inside the body and in the vehicle material double this dose (50 or 100 rem/year during solar maximum or solar minimum years, respectively). Shielding to reduce this overall ionization dosage produced by galactic cosmic rays, say for the solar minimum years when the ionization is higher by a factor of about two, would be a very expensive task in terms of weight. The reason is that shields up to 80 g/cm^2 even of low-Z-number material reduce the dose rate only by a small amount or even increase the dose rate, the latter during solar activity years, when apparently the low-energy part of the primary spectrum is cut off by interplanetary magnetic fields. With such high-energy beams, a buildup of secondaries occurs as has been observed in the atmosphere for a depth of about 60 to 80 g/cm^2 during solar activity years. During minimum solar activity years this transition effect is covered by the ionization produced by low-energy primaries.

Heavy Primary Hits

An important component of the galactic cosmic radiation, namely, the low-energy heavy primaries may be considered separately. As emphasized by Hermann Schaefer, Yagoda, Tobias, Haymaker, and other scientists, the biologically most effective component of the galactic cosmic-ray beam should not be the overall ionization dosage produced in the body but the number of slow heavy primaries, which come to rest by electronic collisions in the unshielded body.

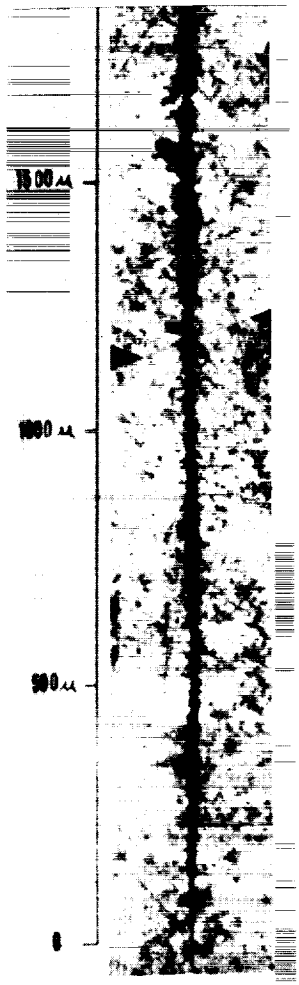

(a) Ionization peak and thin-down part of a heavy nucleus track of $Z \approx 50$ (tin) recorded at 105,000 feet and 55° N latitude with emulsion chamber method, by Herman Yagoda, Laboratory of Physical Biology, National Institutes of Health.

L-62-2051

(b) Microphotograph of two sections of a heavy nucleus track $Z = 20$, and a Thorium alpha track (E. P. Ney and Ph. Freier, University of Minnesota). Left, heavy nucleus of 4,000 million ev energy; center, heavy nucleus at 400 million ev energy; right, thorium alpha track; total vertical length of the visual field, 58 micra.

Figure 5.- Heavy primary tracks in nuclear emulsions.

Figure 5 (ref. 30) shows the ionization spread and thin-down part of such heavy primaries that come to rest by normal ionization without undergoing nuclear collisions, in comparison with the ionization track of a thorium α particle. (See right side of fig. 5(a).) The density of the ionization column around the track increases with Z^2 where Z is the atomic number or charge of the impinging particle. In the core of the column occur doses of 10^4 to 2×10^4 roentgen. The biological effect of such broad columns of ionization with a diameter comparable with the diameter of living cells (10μ) is considered as more profound than the effect which corresponds to their contribution to the overall ionization per volume or gram (the latter is low, approximately 5 percent at the top of the atmosphere). If such a particle traverses on its path sensitive cells, which the body cannot replace, that is, receptor cells of the eye or ear, more serious consequences are anticipated than if the produced ionization is uniformly distributed through the volume, or concentrated on thin tracks. The number of these hits[5] per unit volume of the body is therefore a more adequate measure of their biological effect than their contribution to the dose in rep or rad.

To give an order of magnitude of the number of heavy primary hits on top of the atmosphere, the results obtained during the Man High II balloon flight, August 1957, may be recalled. (See ref. 31.) During a stay of 15 hours at over 90,000 feet altitude (in latitude >55°), the number of calcium (Z = 20) up to iron (Z = 26) hits recorded in three emulsion pellicles 3 × 4 inches × 600μ thick placed on the arms and the chest of the pilot were 3, 1, and 2. The number of lower Z-number hits was in the order of 25 per pellicle. The number of hits (Z > 6) in the whole body during this 15-hour flight is estimated to have been about 150,000 (volume of the body is approximately 75,000 cm^3). Although this total number appears to be high, the number per cubic centimeter is only approximately 2. It was not possible to detect significant biological effects after the flight during subsequent weeks and years of observation. The number of hits/cm^3 that can produce significant effects on man is not as yet clear. At this time one cannot exclude the possibility that the heavy primaries may constitute a radiation danger for expeditions of long duration in a lightly shielded space vehicle. Fortunately, the shielding against low-energy heavy primaries is a easier task than shielding against the high-energy protons and secondaries with low charge. The heavy primaries come to rest by normal ionization in relatively low shield thicknesses because of their high-energy losses, or, if more energetic, convert in nuclear collisions, because of their larger cross sections, into particles of the lightly ionizing type and these have a lower biological effectiveness. Especially favorable in terms of weight for protection against thin-down hits is low-Z-number material, as it is also for protection against protons. Preliminary estimates indicate that a spherical shield having a thickness equivalent to 20 g/cm^2 of H_2O would be necessary to reduce substantially the number of hits in a target like

[5]Called "thin-down" hits because of their arrow shape.

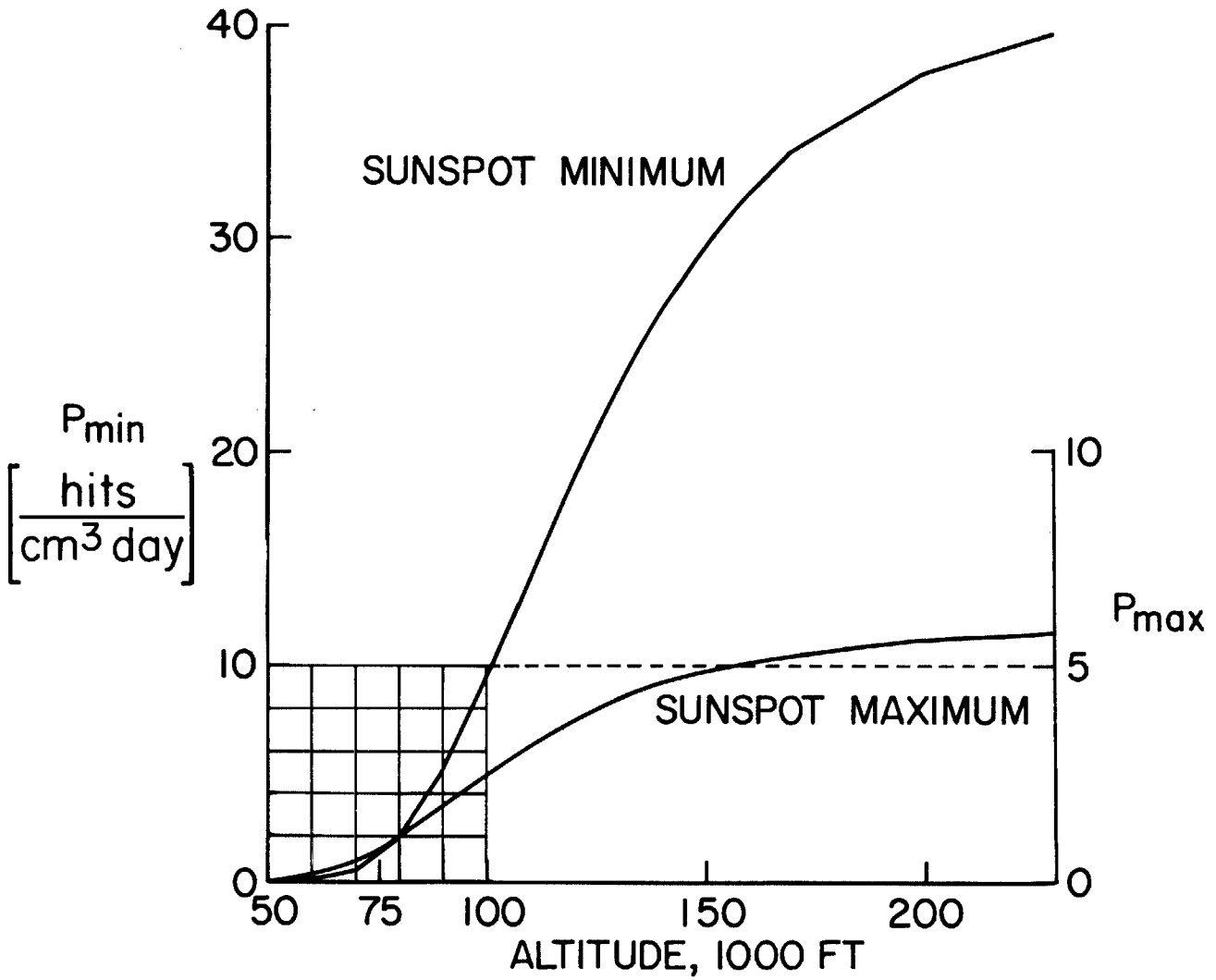

Figure 6.- Variation of thin-down intensities with altitude for seasons of maximum and minimum sunspot activity. (Taken from ref. 32, H. Yagoda.)

man's body. The shielding effect of the atmosphere against heavy primaries can be observed in the curves of figure 6 extrapolated by Yagoda (ref. 32) from careful emulsion measurements in high-altitude balloons in high latitudes. The symbol P denotes the number of hits/cm^3 per day. The number of hits in 20 g/cm^2 depth of atmosphere (87,000 feet or 26.4-km altitude) is reduced by a factor of 8 during solar minimum years and by a factor of 3 during activity years and tends to zero for depths of 40 g/cm^2 in an altitude of about 70,000 feet.

SOLAR COSMIC RAYS

As the third and most important problem, the radiation hazard of energetic solar flare particles has to be considered. This solar cosmic radiation was detected at sea level in some events as early as 1942 by Forbush and Ehmert. Such high-energy proton events that penetrate with their secondaries to sea level are rare. Since the direct measurement of solar protons of lower particle energy in balloons by Winckler in 1957, which are more frequent and are observable only in high altitudes and latitudes, distinction is made between high-energy events with relativistic particle energies up to 20 Bev but having generally lower intensities and duration, and low- and medium-energy events with particle energies up to 400 Mev or few Bev, respectively, in some cases of extreme intensity and duration of the order of 1 week.

Frequencies

The high-energy events until 1959 including one medium-energy event during the three last solar cycles are indicated in figure 7 by the vertical bars. The figure shows furthermore the correlation of flares and sunspot numbers. One or two high-energy events are observed every 4 to 5 years along the rising and falling slope of a sunspot cycle. The most energetic and intensive event since 1938 occurred on February 23, 1956.

The frequency of low- and medium-energy events are shown in figure 8 (modified from fig. 20 of ref. 33; see also ref. 34). The events are indicated by crosses in the figure. About 5 to 13 events occurred per year that were intense enough to be detectable with riometers[6] or in instrumented high-altitude balloons in high latitudes. Most of these low-energy events do not constitute a danger in a space vehicle shielded by about 5 to 10 g/cm^2 of low-Z-number material because of their low intensity.

---

[6]Radio ionospheric opacity meter: measures the cosmic radio noise absorption at 28 and 50 Mc in the lower ionosphere (30 to 100 km) caused by penetrating ionizing particles and protons.

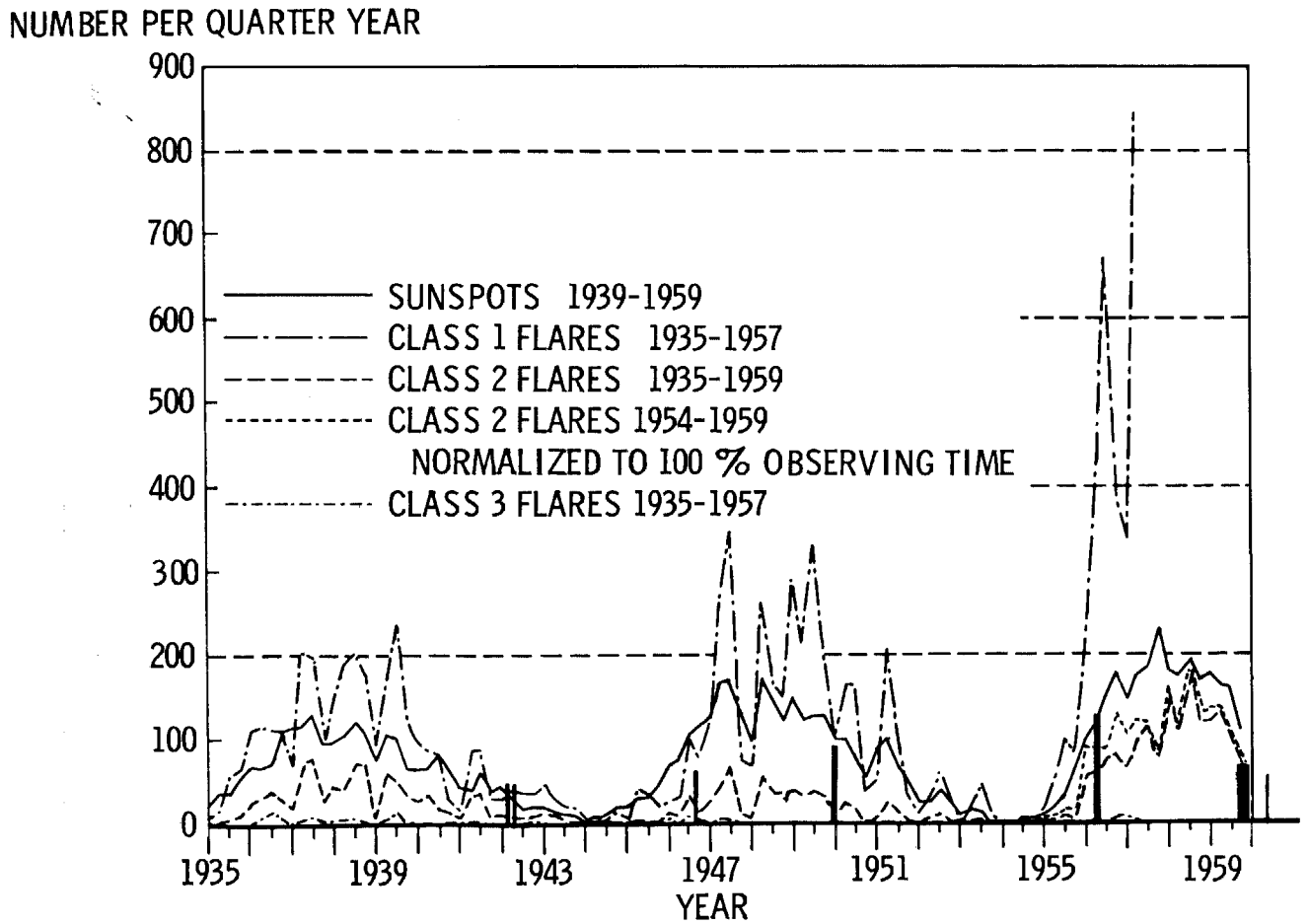

Figure 7.- Frequencies of sunspots and flares in the last solar periods and high-energy proton events. (Courtesy J. W. Evans, Sacramento Peak Observatory, New Mexico.)

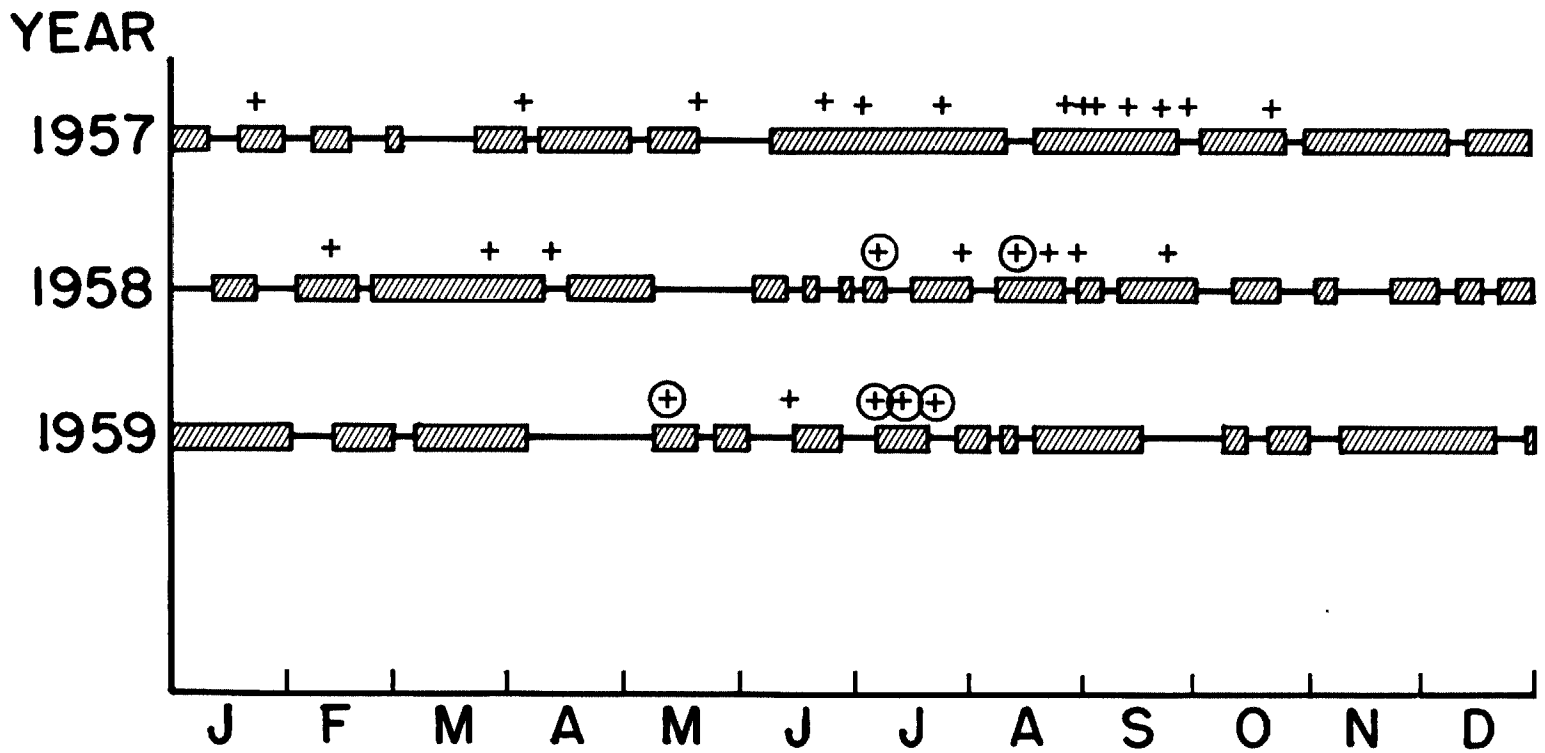

Figure 8.- Frequency of low- and medium-energy solar events and correlation with large penumbral areas of sunspots.

Extreme flux low- and medium-energy events, which produce a radio attenuation of 15 decibels and more (28 Mc) constitute, however, an appreciable hazard (indicated by circles in fig. 8). Of such extreme events only 2 to 4 per year occurred during the last years of high solar activity. Of course, sometimes 2 or more occurred in very short succession within a few days, like the events on July 10, 14, and 16, 1959 and the events on November 10, 12, and 15, 1960.

Prediction of Quiet Periods and Encounter Probabilities

A second purpose of figure 8 is to indicate a correlation between occurrence of penumbral areas around sunspot groups that exceeded a critical area and proton events, a correlation used by Anderson for prediction purposes (ref. 33). These times of large penumbras are indicated by hatched boxes. In all except two instances no solar events occurred during periods of absence of large penumbral areas; and when such events occurred, they were not earlier than 2 days after the increase of penumbral areas. On the basis of Anderson's analysis of the years 1957 to 1959 it appears that absence of major events can be predicted for excursion times of 2 to 4 days with acceptable reliability from observation of sunspot groups. For excursions of 7 days or more, however, the probability of encountering a strong event increases rapidly. The possibility of developing methods that reliably predict longer quiet periods in the order of 10 to 14 days duration on the basis of penumbra or magnetic observations on sunspot groups appears to be low to astronomers at present. The reason for this view is in part a proton-producing flare occurring on September 30, 1961, which occurred in an unsuspicious region without sunspot groups and the rapid changes which the sunspot groups undergo.

On a purely random statistical basis of occurrences, the probability of encountering an extreme event in a 10-day trip would be $\frac{4}{36.5} = 0.11$ or 11 encounters in 100 flights, four extreme events per solar activity year being assumed. The probability of encountering two events or more would be 0.006 or 0.6 percent. It should be noted, however, that these events tend to occur in bunches. By investigation of the last three solar cycles, on the basis of a correlation between flare events and large magnetic disturbances as measured by a magnetic index $A_p > 80$, Adamson and Davidson (ref. 35) found that the bunching effect diminishes the probability for one event by a factor 0.8 and increases the probability for two or more events in a 10-day excursion by a factor >2 to about 1.2 percent. These encounter probabilities for short-time excursions are considered as too high to be ignored and, as long as no reliable prediction criteria are found, an amount of shielding is recommended that reduces the dose accumulated in two or three events to tolerable limits even for expeditions of only 10 to 14 days duration in space. Adequate shielding appears to be indispensable for excursions of longer duration

during solar activity years, such as a Mars expedition, which would take more than a year.

Maximum Fluxes and Spectra

To obtain a survey about dose rates and doses and shielding requirements, it is necessary again to know the fluxes and the spectra, and equally important, their variations with time especially during the maximum intensity phases of such proton events.

Referring to maximum intensities, it is known that the fluxes of energetic protons of various events vary in wide limits - by about six orders of magnitude - from cosmic-ray background intensity of 2.5 protons/cm^2-sec, corresponding to a dose rate of 0.1 rad/week up to possibly 10^6 protons/cm^2-sec, corresponding to up to thousand rad/hour behind a small amount of shielding. To obtain upper limits of doses only fluxes and spectra of the most extreme events observed in the last solar cycle, as given in figure 9 are considered.

The fluxes of particles having energies $>E$ are plotted against the energy E in Bev on the abscissa. These spectra have a common characteristic, they fall off much more steeply in the high-energy range than the spectra of the inner belt protons or of galactic cosmic protons. This characteristic leads to the expectation that, with practical shielding amounts in the order of 30 g/cm^2, the main intensity can be cut off, at least for low- and medium-energy events. For example, in the May 1959 low-energy event after 33 hours using a 30 g/cm^2 H_2O shield corresponding to the range of 220 Mev protons, only approximately 100 protons/cm^2-sec sterad with $E > 220$ Mev penetrate the shield; the 10^4 times higher flux of particles $E < 220$ Mev is absorbed in the shield.

During the high-energy event on February 23, 1956, however, only a small - of course, not insignificant - part of the spectrum could have been cut off by the shielding amount of 30 g/cm^2. The steep decrease of the spectrum begins not earlier than at approximately 1 Bev and it is necessary to use a water shield of 3 meter thickness to cut off all particles with lower energy. The shielding effect of even 3 meters of H_2O is still overestimated based on these electronic collision range considerations. The fact is disregarded that most of the protons would undergo nuclear collisions producing secondary protons, neutrons, and mesons, which penetrate in part even farther and produce further penetrating secondaries by decay or nuclear reactions.

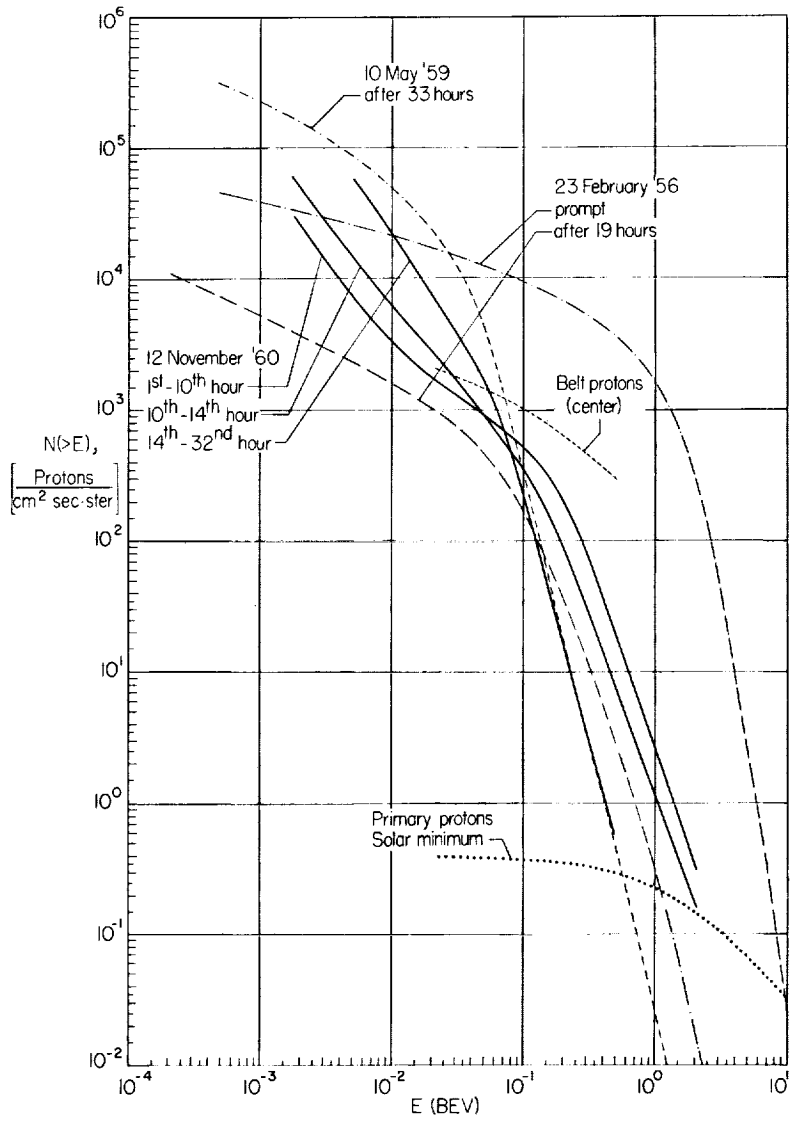

Figure 9.- Integral energy spectra of solar flare cosmic rays, inner belt protons, and galactic primary protons. The spectra of February 1956, May 1959, and of galactic cosmic rays are plotted against energy from the rigidity spectra given by Winckler (ref. 6) and Bailey (ref. 9). The spectra of November 12, 1960 are extrapolated from spectra given by Fichtel and Guss (personal communications) and measurements of Davis and Olgivie (personal communications), Van Allen (Explorer VII, personal communications), Winckler (ref. 8), and Ney (ref. 36). The inner belt proton spectrum (center) is obtained from Freden and White's spectrum in 1,200-kilometer altitude (ref. 2) by multiplication by 20.

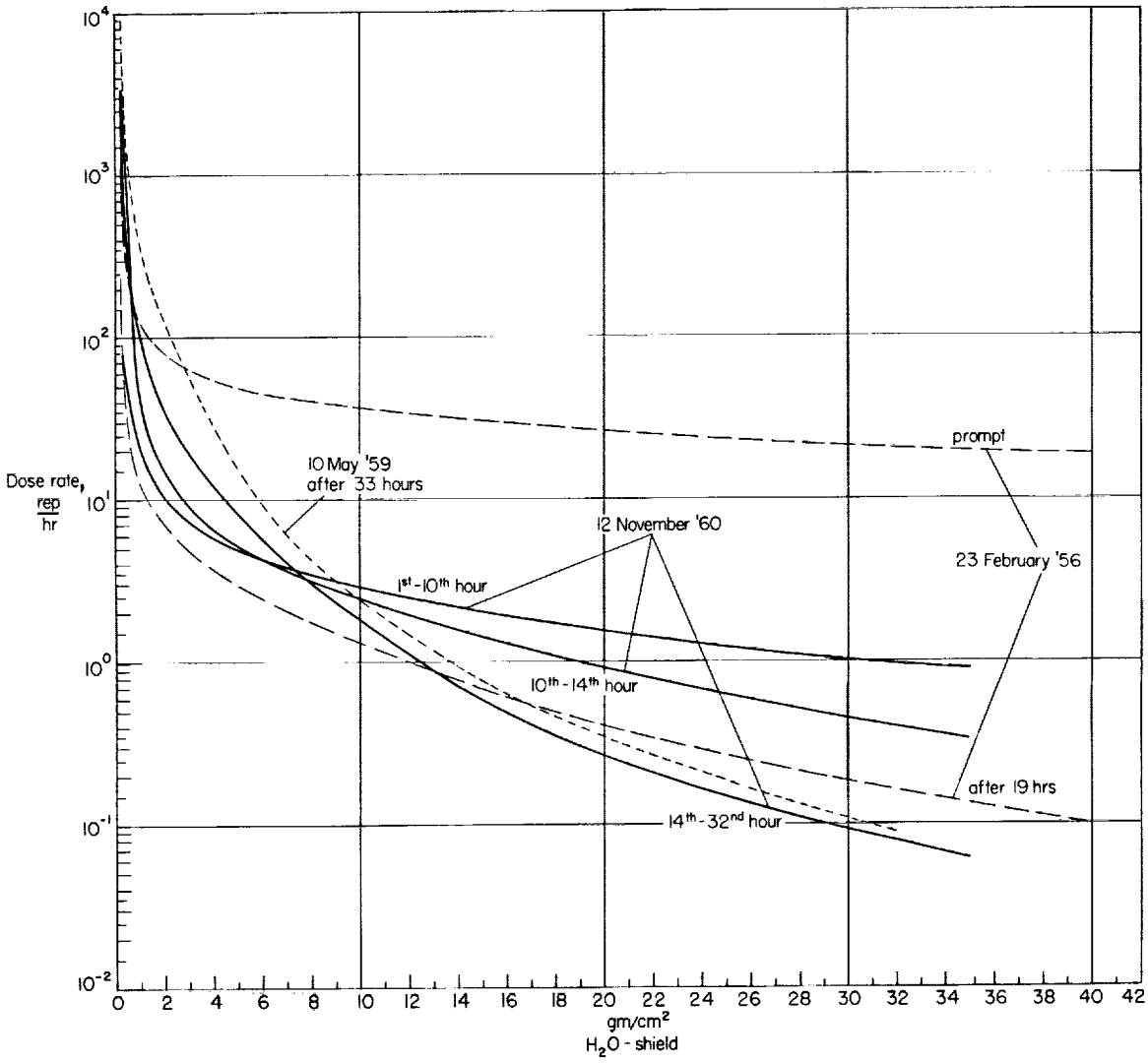

Figure 10.- Proton dose rates in the center of spherical shields derived from the spectra in figure 9.

Dose Rates and Upper and Lower Limits of Doses

From these spectra the dose rates beneath various shielding thicknesses at that particular instant for which spectrum is given can be approximately calculated. (See appendix.) Qualitatively, the different penetration power of solar beams can be seen in figure 10, which shows the slower decrease of the dose rate with increasing shielding thickness in high- and medium-energy events in comparison with the fast decrease in low-energy events, neglecting secondary production, and assuming that all protons are slowed down by electronic collisions only. (See also refs. 7 and 37.)

For estimating the radiation hazard of such proton events it is, however, necessary not merely to consider the dose rate as a function of shielding thickness but the time-integrated dose rate or the total dose accumulated during the entire event rather than the dose rate at particular instants. The biological effect is measured by the dose itself. For accomplishment of these dose calculations it is necessary to know the variation of the spectra with time or the time profiles of intensities of particles above the various energies.

Each of these proton events has its own - often complicated - time history of intensities and spectra dependent on the source spectrum on the sun and magnetic fields between sun and earth. Frequently, rapid increase is followed first by a fast and later by a slow decrease of the intensity as shown in figure 11 (ref. 38). The surge of secondary neutrons at sea level in figure 11 reflects, of course, only the intensity of the high-energy protons ($E > 1$ Bev) on top of the atmosphere.

The increase and 50-percent decay period varies in duration from some 10 minutes (fast riser) to 24 hours (slow riser) in different events. Sometimes multiple peaks appear in the early phase. This effect is seen in figure 12 (from ref. 39), which shows the slow neutron increase during the November 12, 1960 event.

Unfortunately, the intensities and the spectra during these early phases of maximum intensity that contribute most to the dose are not well known in many cases. For this reason, in figure 13 only rough estimates of upper and lower limits of doses in the various events can be given. These estimates are derived (see also ref. 7) on the basis of the spectra, extrapolated in part, in figure 10 and time profiles of intensities extrapolated from neutron monitor, riometer (see ref. 40), balloon (refs. 8 and 36), rocket[7] (refs. 41 and 42), satellite (Explorer VII), and space probe measurements (Pioneer V, ref. 6) as described in the appendix.

---

[7]See also: Novick, D., ed.: Minutes of Meeting NASA Advisory Committee on Nuclear Energy Systems. NASA Marshall Space Flight Center (Huntsville, Ala.), May 1961. (Not generally available.)

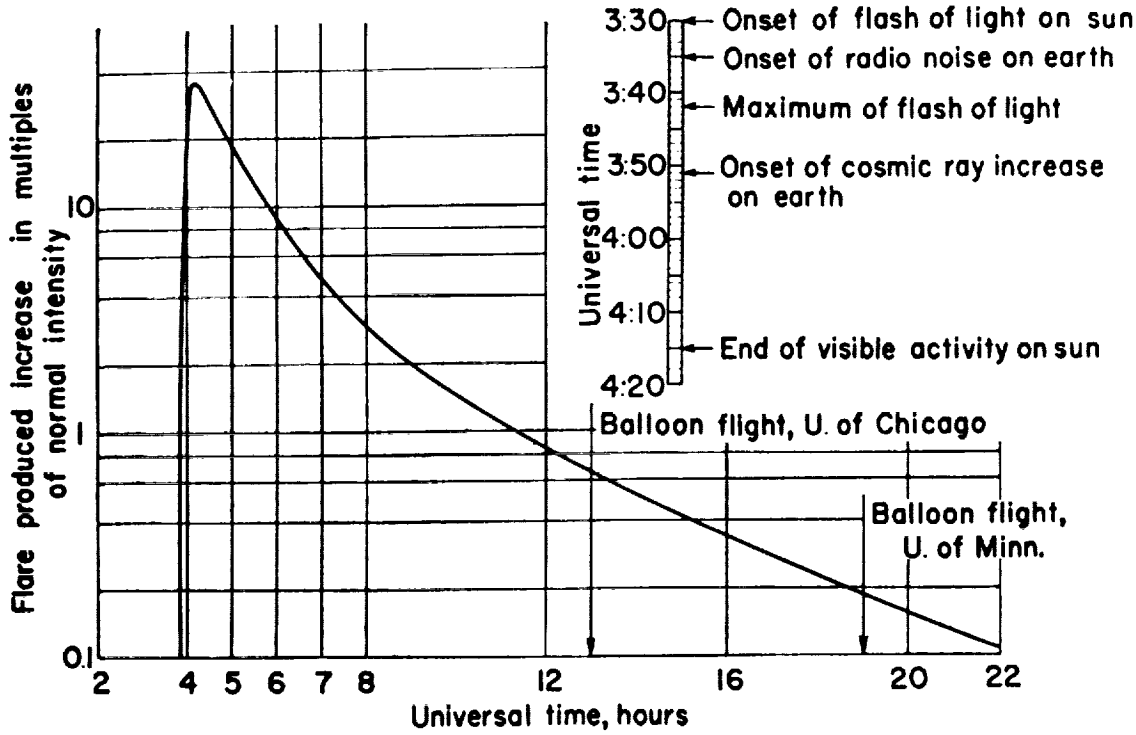

Figure 11.- Cosmic-ray neutron surge at sea level during large solar flare of February 23, 1956. Observed by Lockwood et al. at Durham, New Hampshire. (Reproduced from ref. 38.)

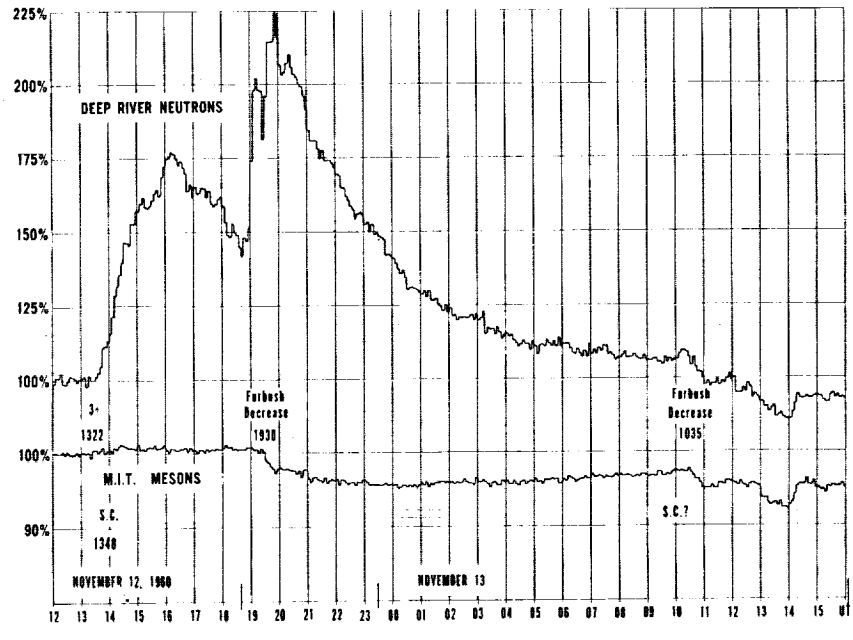

Figure 12.- Neutron surge at sea level in Deep River, Canada from November 12 to November 15, 1960 and meson decrease measured at Massachusetts Institute of Technology. (J. F. Steljes, H. Carmichael, and K. G. McCracken, ref. 39.)

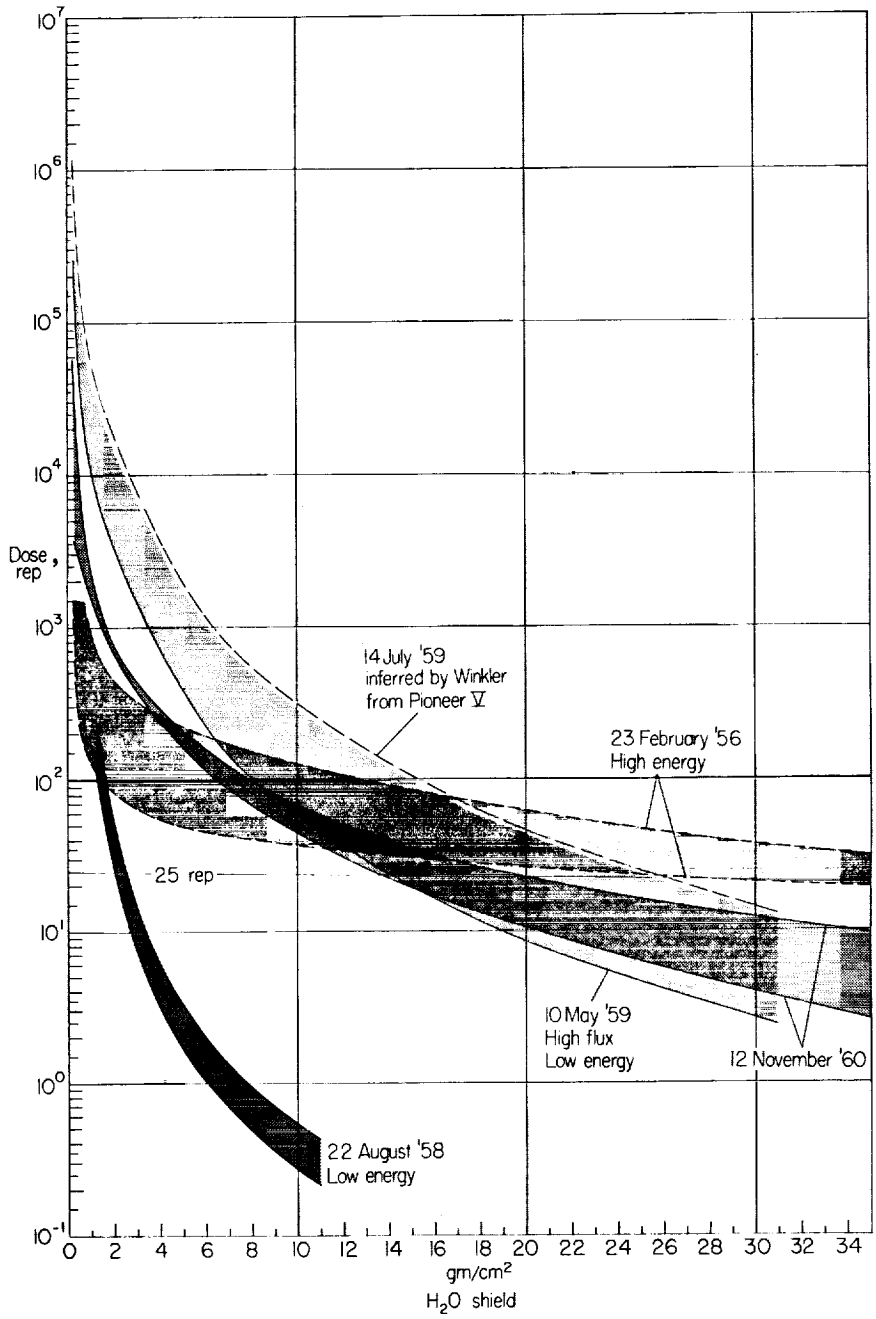

Figure 13.- Estimates of upper and lower limits of doses in the center of spherical H_2O shields accumulated during extreme proton events.

Note some dose values, as follows: Behind a shield of 2 g/cm^2 of H_2O a dose in the 1,000 rep range could possibly be received; behind a shield of 25 g/cm^2 of H_2O, the dose would be reduced to an upper limit of 50 rep in the high-energy event of February 1956. In the low- and medium-energy events the upper limit would be below 25 rep behind a shield of 25 g/cm^2 of H_2O.

It should be mentioned that the upper limits of doses for the May and July 1959 events and for the February 1956 high-energy event are probably assumed to be unnecessarily high. (See ref. 6.) These values are more uncertain than the values given for November 12, 1960, where more spectra are available. It is, however, obvious that operating during such events in a lightly shielded space vehicle or staying on the moon surface protected only by a space suit for extended periods would be dangerous, since radiation sickness can be expected at doses of 150 to 200 rem.

These considerations may be summarized with the statement that about 25 g/cm^2 of H_2O equivalent shielding would be sufficient to reduce the exposure of the crew to 25 to 50 rep for every extreme event observed thus far. If two or three encounters are considered, total shield weights of 20 to 25 g/cm^2 of H_2O would maintain the sum of the doses from the encounters at less than 100 rep. These estimates include in the author's opinion a substantial safety margin, since no self-shielding is taken into account and since, furthermore, the spectra for solar proton events and the time profiles of intensities used here are upper limits.

Of course, the question of contribution of secondaries, especially neutrons behind large shield thicknesses, to the dose has to be investigated in more detail. A rough estimate (ref. 7), using the prompt spectrum of the February 23, 1956 high-energy event, shows that the contribution of neutrons to the physical dose rate in rep/hour is about 15 percent behind a shield of 25 g/cm^2 of H_2O. However, the contribution of secondary neutrons to the biological dose in rems should be higher and has to be taken into account for low-energy events, too, which apparently can exhibit extreme proton fluxes in the low-energy range with subsequent neutron and γ-fluxes that cannot be ignored. Approximate calculations in reference 43 show that in low-energy events such as that of May 1959 inside aluminum of thickness >20 g/cm^2 the contribution of secondary neutrons to the rad dose would be about 40 percent, inside H_2O less than 20 percent.

SUMMARY OF RESULTS AND CONCLUDING REMARKS

Galactic cosmic radiation constitutes a comparatively minor hazard insofar as the overall ionization dosage is concerned. At the low level

of 0.5 rem/week or 1 rem/week during solar activity years, it has significance only on a trip of extended duration. In 1 to 2 years a dose of about 50 to 100 rem would be accumulated in a space ship during solar activity years. In adding up this amount of chronic low-level irradiation to other more acute doses associated with belt and flare radiations, it is necessary to apply a reduction factor to the galactic dose because of recovery of somatic damage, except for genetic effects, which are, however, considered as insignificant for doses in the order of 50 to 100 rem for one generation.

The effects of certain secondary components and of the heavy primary component of the cosmic-ray beam at long-term low-level exposure are not definitely known at present. The number of heavy primary hits without any shielding in free space is low, on the order of 6 to 40 per cubic centimeter of tissue per day. It cannot be excluded that staying without substantial shielding for months in space would lead to injury. Fortunately, shielding in the order of 30 g/cm^2 of low-Z-number material would reduce the number of heavy primary hits by a factor 15 or 4 during solar minimum or solar activity years, respectively. The number of hits decreases fast to zero with higher shield thicknesses; these thicknesses should be available in the form of propellant and supplies for long-term excursions.

The radiation of the earth radiation belts, although of 10^4 times higher proton intensity in the center of the inner belt, is nevertheless no major hazard if the vehicle crosses the critical part of the inner belt in 10 minutes, as was done by Pioneer III and IV. The proton dose is estimated to amount to only 3 to 6 rad for exit and return through the center in a lightly shielded vehicle. The secondary X-radiation from the belt electrons is probably held substantially below the level of 1 to 2 rem/hour by the normal content of low- and high-Z-number material of the walls of a typical vehicle, especially if these walls are covered by low-Z-number material on the outside.

The most serious radiation problem for longer excursions into space during solar activity years is apparently posed by solar-flare proton events. The potential radiation hazard depends on the date of the excursion. During solar minimum years no flares of importance are observed for more than a year. During solar activity years, even for excursion times of only 10 to 14 days, the probability of encountering an extreme event is not a negligible quantity. The absence of such events for such periods can also not be predicted from synoptical observations of solar phenomena with acceptable reliability at present. Adequate shielding for excursions of the order of weeks is recommended and becomes a necessity for trips of longer duration during solar activity years.

Upper and lower limits of doses as functions of shielding thickness are given in table I. Since more data have become available, especially about the intensities in the early phases of these events, it would appear that the upper limit of proton rad doses given in this table are unnecessarily high in some events. From calculations to date, it appears that in first approximation these upper limits may be considered as rem doses, including the contribution of secondaries, especially neutrons, to the biological dose, with the reservation that the shielding material has to be appropriately selected on the basis of detailed investigations. Based on these upper limits the result is obtained that shielding equivalent to 25 g/cm^2 of H_2O would have been sufficient for reducing the dose to 25 rem for every extreme low- or medium-energy event observed so far and for reducing the dose to 50 rem in passing through the event of February 23, 1956, the most intense high-energy event of the last two solar cycles. With respect to the radiation hazard during excursions with a duration of weeks or more, it must be remembered that two or three solar proton events of comparable intensity frequently occur in short succession; therefore, the accummulated dose with shielding of 25 g/cm^2 would increase to 75 to 100 rem. For long-term excursions due to the contribution of galactic cosmic rays, even heavier shielding may be necessary to reduce the contribution of flare events.

According to these preliminary estimates the radiation problem in space appears to be more serious than was suspected even 5 years ago, as Alvin M. Weinberg of the Oak Ridge National Laboratory has emphasized. (See ref. 44.) The feasibility of longer excursions also during solar activity years appears, of course, not questionable. If supplemental shielding is provided by appropriate positioning of equipment and supplies, the necessary additive weight for individual shielding should hardly surpass 25 percent of the space-vehicle weight as it is envisioned even for smaller vehicles without regard to shielding.

Langley Research Center,
National Aeronautics and Space Administration,
Langley Air Force Base, Va., March 12, 1962.

TABLE I.- ESTIMATED RADIATION EXPOSURE IN SPACE

(a) Galactic cosmic radiation

	Gross ionization dosage	Heavy primary hits	
		Without shield	20 g/cm^2 of H_2O
During solar activity years	0.45 to 1.0 rem/week 25 to 50 rem/year	6/cm^3/day	2/cm^3/day

(b) Belt radiation

Shield thickness	Inside spherical shields, neglecting self-shielding		
	2 g/cm^2 of H_2O	6 to 10 g/cm^2 of Al + steel	25 g/cm^2 of H_2O
Inner belt protons (center)	12 to 24 rad/hr	----------	2.7 to 5.4 rad/hr
Outer belt electrons (center) X-radiation	----------	<2 rem/hour	----------

(c) Solar cosmic radiation

	Inside spherical shields, neglecting self-shielding	
	2 g/cm^2 of H_2O	25 g/cm^2 of H_2O
Low energy, extreme flux, May, July 1959	2,500* to 15,000* rad	6 to 25 rad
Medium energy, extreme flux, November 1960	600 to 800 rad	6 to 19 rad
High energy, high flux, February 1956	80 to 400* rad	25 to 50* rad

*These values are extrapolated and highly uncertain.

APPENDIX

CALCULATION OF PROTON DOSE RATES AND DOSES IN THE CENTER OF SPHERICAL SHIELDS

Definition of Dose Units and Terms Used in Radiobiology

The following definitions of dose units and radiobiological terms are used:

r (roentgen): 1 r is the amount of X-radiation which produces 2.08×10^9 ion pairs (one electrostatic unit of charge) per cubic centimeter of standard air (energy absorption, 83.7 erg/g air). This amount of X-radiation deposits, however, in 1 gram of material of higher Z-number (for example, bone) much more energy than in 1 gram of soft tissue, water, or air, especially if the X-radiation is soft. Since the amount of energy absorbed per gram or the number of ion pairs per gram is in first approximation a measure of the biological effect, at present simply the absorbed energy per gram produced by any kind of radiation (also particle radiation) is commonly used as a measure of the physical dose. Its units are rep or rad.

rep (roentgen equivalent physical): 1 rep is defined here as 93 erg/g absorbed energy. This energy is absorbed by 1 gram of soft tissue or water exposed to 1 roentgen of X-radiation ($E \geq 200$ Kev).

rad: 1 rad = 100 erg/g absorbed energy.

RBE (relative biological effectiveness): Low-energy protons ($E < 15$ Mev), α and heavier ions, which ionize more densely along their paths have generally a higher biological effect than X-radiation at the same ionization or energy absorption per gram, that is, at the same rep or rad dose. Hence, for particle radiation this physical dose has to be multiplied by the RBE factor which is dependent not only on the specific radiation, but also on the specific effect and organ in question, and on the mode of application, to obtain the biological dose in rem (roentgen equivalent men).

$$\text{Dose in rem} = \text{Dose in rep (or rad)} \times \text{RBE}$$

The RBE factor can have values from 1 to 15, the latter for relatively slow heavily charged particles. The RBE of penetrating high-energy proton beams in the energy range 10 Mev to 1 Bev, which are mainly of concern in space vehicles, have in general only an RBE $\leqq 1.5$ because of their low specific ionization. This value refers to bone marrow, intestinal, and general somatic damage, if secondaries can be ignored. Special attention has to be given to the eyes so that they are not exposed to low-energy protons and fast neutrons.

dose limits: An acute total body dose of 450 rem is lethal for 50 percent of men exposed and is designated as LD50. Other doses are defined as follows:

150 to 200 rem: average acute total body dose for radiation sickness.

80 to 100 rem (acute, total body): "critical dose" produces light symptoms of the acute syndrome for 5 to 10 percent of those exposed to it in a period of about 1 day or shorter.

Symbols

Z	atomic number of nuclei or positive charge in elementary units
E	kinetic energy of particles in ev (1 ev = 1.6×10^{-12} erg; Kev = 10^3 ev; Mev = 10^6 ev; Bev = 10^9 ev)
P	number of hits per cubic centimeter emulsion per day
t	time, sec
R	ranges of protons in matter, assuming electronic collisions only, in g/cm^2
$\dot{N}(>E)$	number of particles having energies $>E$, which arrive per unit time isotropically from a solid angle 1 steradian or 4π and penetrate a sphere of 1 cm^2 cross section. This number of particles/cm^2-sec-ster or particles/cm^2-sec, respectively, as a function of energy is called "integral energy spectrum."
$\dot{N}'$	number of protons/cm^2-sec per unit range (g/cm^2); as function of range called "differential range spectrum," $d\dot{N}/dR$
x	thickness of shield in g/cm^2
S	linear energy loss per unit mass (proportional to specific ionization) or mass stopping power, Mev/g/cm^2

k dimension constant

D dose, see units defined in preceding section

Subscripts:

max maximum value

min minimum value

0 initial conditions

Dots over symbols denote derivatives with respect to time.

Dose-Rate Calculations

The contribution to the physical dose rate behind a plane shield of thickness x g/cm^2 from a parallel beam of $\dot{N}'(R)dr$ protons/cm^2-sec having a range between R and $R + dr$ g/cm^2, nuclear reactions being neglected, is given by

$$dD(x)\left(\frac{rep}{hr}\right) = k \cdot S(R - x) \cdot \dot{N}'(r)dR$$

as seen in figure 14, or

$$dD(x)\left(\frac{rep}{hr}\right) = 1.25 \cdot 10^{-4} \cdot \frac{S(R - x)}{S_{min}} \cdot \dot{N}'(R)dR$$

Here $S(R - x)/S_{min}$ is the energy loss $S(R - x)$ of protons of the range $R - x$ over the constant minimum energy loss S_{min} of protons of relativistic energies (2 Bev), for example, in water.

$\dot{N}'(R) = \frac{d\dot{N}}{dR}$ is the flux of protons of range R in $\left(\frac{\text{protons}}{\text{cm}^2\text{-sec} \cdot \text{g/cm}^2}\right)$

The physical dose unit 1 rep (roentgen equivalent physical) is defined as 93 erg absorbed energy per 1 gram, which corresponds to the energy absorbed in 1 gram water at an amount of X-radiation of 1 roentgen and is substantially the same as the more modern unit 1 rad = 100 erg/g. The dimensional factor $k \cdot S_{min} = 1.25 \cdot 10^{-4}$ is obtained by transition from Mev/g and from seconds to rep units and hours $\left(S_{min} = 2.0 \frac{\text{Mev}}{\text{g/cm}^2} = 2.0 \cdot 1.6 \cdot 10^{-6} \frac{\text{erg}}{\text{g/cm}^2} = \frac{2.0 \cdot 1.6 \cdot 10^{-6}}{93} \text{ rep-cm}^2$ has to be multiplied by 3,600$\right)$.

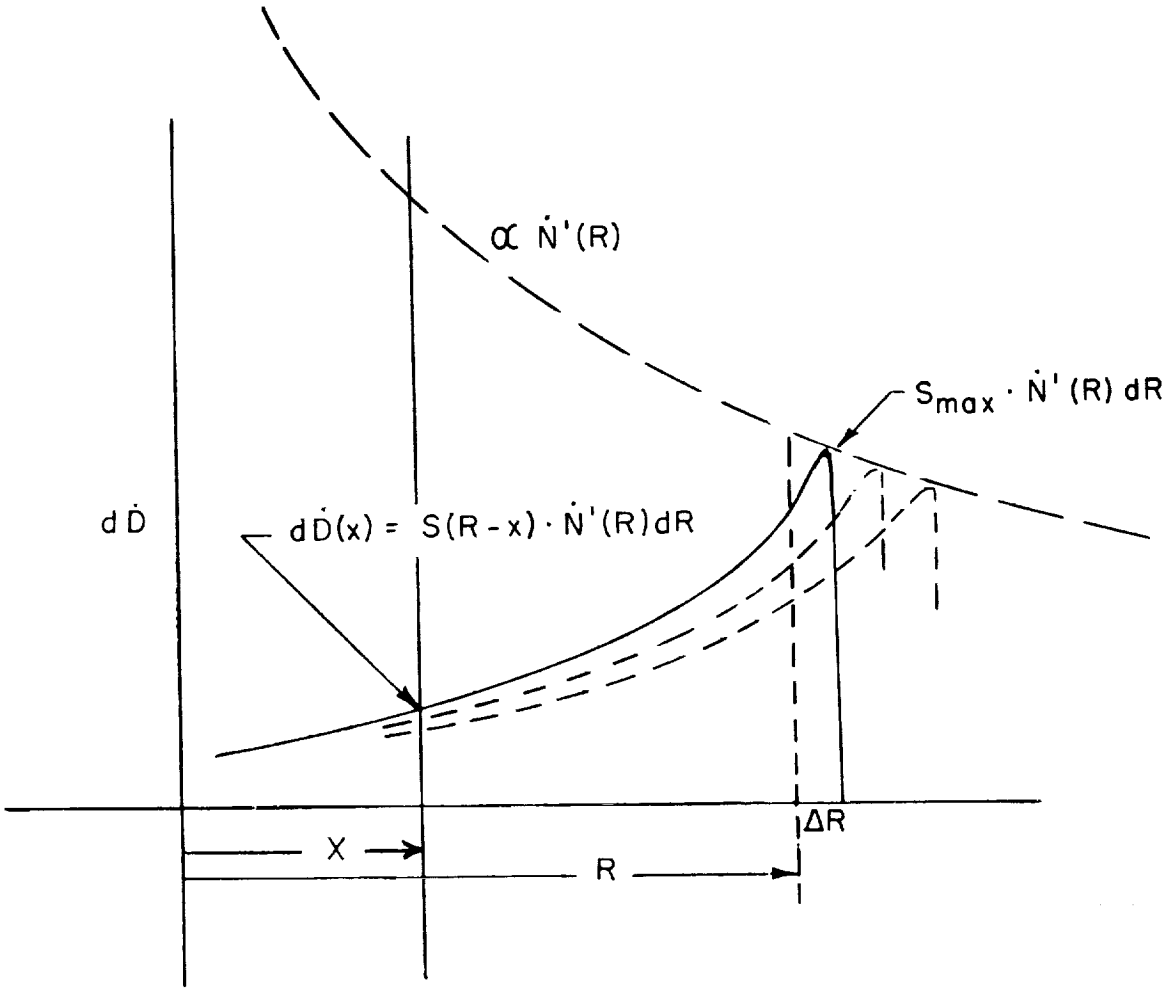

Figure 14.- Dose rate behind a shield of thickness x is obtained by summarizing the contributions of all particles with range $R > x$.

If there is an omnidirectional isotropic flux of $\dot{N}'\left(\frac{\text{protons}}{\text{cm}^2\text{-sec-g/cm}^2}\right)$, a sphere of cross section 1 cm^2 in the center of a spherical shield of thickness x receives correspondingly a dose rate of:

$$\dot{D}(x)\left(\frac{\text{rep}}{\text{hr}}\right) = 1.25 \cdot 10^{-4} \int_{R=x}^{R=\infty} \frac{S(R - x)}{S_{min}} \dot{N}'(R)\,dR \qquad (1)$$

The integral is replaced in the numerical calculations by

$$\sum_{R=x}^{\infty} \frac{\overline{S}\left(\begin{matrix} R - x \\ R + dR - x \end{matrix}\right)}{S_{min}} \dot{N}'\left(\begin{matrix} R \\ R + dR \end{matrix}\right) \cdot dR$$

where $\overline{S}/S_{min}$ is obtained from the energy loss or stopping power formula for water. (See fig. 15; refs. 45 to 47.) The stopping power and curves of range plotted against energy for iron in figures 15 and 16 are taken from the energy-loss-momentum and range-momentum curves (ref. 47, pp. 38 and 44) by replacing momentum by energy on the abscissa.

The steps dR are taken as small as 50 mg/cm^2 for small R - x, because of the very steep increase of S for small arguments. The summation was extended up to R = 500 to 1,000 g/cm^2 for low- and high-energy events, respectively.

The differential range spectra $\dot{N}'(R)$ are derived from the integral energy spectra figure 9 by numerical differentiation and multiplication with the factor dE/dR (fig. 15, water) as follows:

$$\frac{d\dot{N}}{dR} = \frac{d\dot{N}}{dE} \cdot \frac{dE}{dR}$$

Formula (1) can be written in the form (this form is found in ref. 1, Van Allen and Frank):

$$\dot{D}(x)\left(\frac{\text{rep}}{\text{hr}}\right) = 1.25 \cdot 10^{-4} \left(\overline{\frac{S}{S_{min}}}\right)_x \cdot \dot{N}(x)\left(\frac{\text{protons}}{\text{cm}^2\text{-sec}}\right) \qquad (2)$$

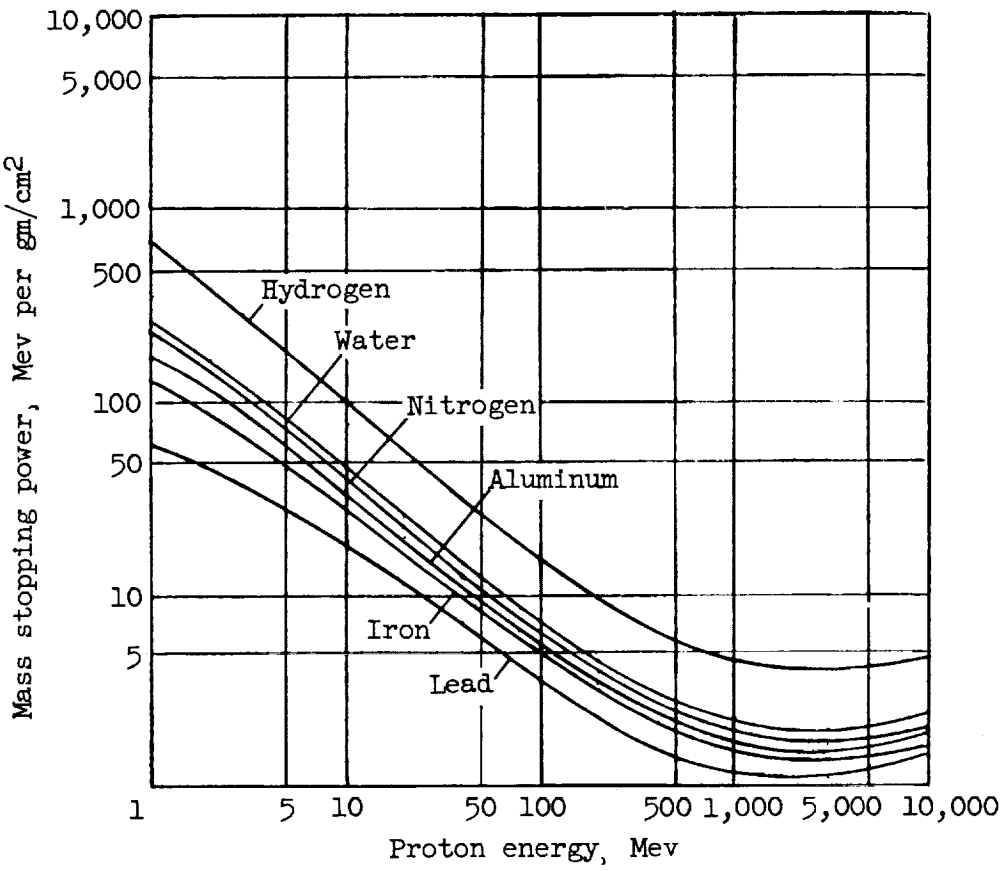

Figure 15.- The mass stopping power of protons for different materials as a function of proton energy.

Here the $\dot{N}(x) = \int_{R=x}^{\infty} \dot{N}'(R)dR$ protons/cm^2-sec penetrating the shield thickness x can be read directly from the respective integral energy spectrum of figure 9 (ordinate to be multiplied by 4π to include complete sphere) and by using the range energy relation of figure 16.

The average relative energy loss of these $\dot{N}(x)$ penetrating protons is defined by

$$\left(\overline{\frac{S}{S_{min}}}\right)_x = \frac{\int_{R=x}^{\infty} \frac{S(R-x)}{S_{min}} \dot{N}'(R)dR}{\int_{R=x}^{\infty} \dot{N}'(R)dR} \qquad (3)$$

The calculation of $\left(\overline{\frac{S}{S_{min}}}\right)_x$ is tedious because for each x an integration has to be performed over the product $\frac{S(R-x)}{S_{min}}\dot{N}'(R)$. The range of its values dependent on the differential range or energy spectrum may therefore be indicated. $\frac{S(R-x)}{S_{min}}$ decreases from 125 to 1 if the penetrating protons vary in their energy from 1 Mev to relativistic energies (>1,000 Mev), but only from 7 or 3 to 1, if only the penetrating protons $E > 40$ Mev or $E > 100$ Mev, respectively, are considered. If the percentage of low-energy protons ($E \leq 40$ Mev) after penetration is small, as it is the case behind some g/cm^2 shielding, the average S/S_{min} lies between 8 and 1.

For a rough survey the approach

$$\left(\overline{\frac{S}{S_{min}}}\right)_x = \frac{S(x)}{S_{min}}$$

may be used by taking into account the hardening of the penetrating radiation with increasing shield thickness. Here $S(x)$ means the energy loss of protons at an energy corresponding to a residual range x, for example, $x = 2$ g/cm^2, $E = 42$ Mev yields $S(x)/S_{min} = 15/2 = 7.5$. (See figs. 16 and 15.) For a spectrum that falls off steeply ($\approx E^{-4}$ to

E^{-5}) as that of November 12, 1960, during fourteenth to thirty secondth hour after the flare (see fig. 9), this approach is about right for $x = 2$ g/cm^2 thickness; however, it is too low by a factor 3 for large shield thicknesses (25 g/cm^2). For a spectrum that is flat in the tenth and hundredth Mev range as is the prompt spectrum of February 23, 1956 ($\approx E^{-1}$ to E^{-2}, fig. 9), this approach results in a dose rate, which is too high by a factor 2 for low shield thicknesses (2 g/cm^2) and about right for shield thicknesses of the order of 25 g/cm^2.

Calculation of the Doses

The time-integrated formula (1) using the time unit seconds on both sides can again be written

$$\boxed{D(x)(\text{rep}) = 3.5 \cdot 10^{-8} \left(\overline{\frac{S}{S_{min}}}\right)^t_x N(x)} \qquad (4)$$

Here $N(x) = \int_{R=x}^{\infty} N'(R)dR$ is the omnidirectional flux (protons/cm^2) integrated over all ranges $>x$ or energies $>Ex$ and over the time and can be read from the time-integrated integral energy spectrum.

The time-integrated average relative energy loss

$$\left(\overline{\frac{S}{S_{min}}}\right)^t_x = \frac{\int_{R=x}^{\infty} \frac{S(R-x)}{S_{min}} N'(R)dR}{\int_{R=x}^{\infty} N'(R)dR}$$

where $N'(R)dR = \int_0^t \dot{N}'(R)dR\,dt$ are the number of protons accumulated with time between R and $R + dR$ is the same as that given in formula (3), if the spectrum does not change in its shape with time. Otherwise, the time-integrated differential range spectrum $N'(R) = \int_0^t \dot{N}'(R)dt$ where N' has the dimension $\frac{\text{protons}}{\text{cm}^2\text{-g/cm}^2}$ has to be used for calculation of $\left(\overline{\frac{S}{S_{min}}}\right)^t_x$.

The range-energy curves (fig. 16) are deduced from the stopping power formulas (fig. 15) with theoretical values of the average excitation potential I (Bethe, Livingston, F. H. Smith, and Bloch) by integration of the reciprocal of the rate of energy loss with respect to the energy. (See refs. 45 to 47.)

These range-energy curves indicate that the range of protons of energies between 40 Mev and 500 Mev in other materials than water differs only by an energy-independent factor.

The abscissa in figures 10 and 13, the graphs which indicate the dose rate or dose on the ordinate, secondaries being disregarded, has to be expanded or contracted by this factor. That means that the equivalent shielding weight in g/cm^2 of other material is obtained by multiplication of the water value by this factor. For examples, see following table:

Element	Multiplication factor	25 g/cm^2 H_2O corresponds to -
Hydrogen	0.55	13.8 g/cm^2 H
Aluminum	1.37	33 g/cm^2 Al
Iron	1.7	42.5 g/cm^2 Fe
Lead	2.5	62 g/cm^2 Pb

Calculation of the Upper and Lower Limits of Solar Flare Doses in Figure 13[8]

In figure 13 three kinds of extreme proton events are considered: low-energy events, high-energy events, and medium-energy events.

Low-energy events (Aug. 22, 1958; May 10, 1959; July 14, 1959).- In these low-energy events only the spectra at a time 14, 33, and 21 and 31 hours, respectively, after the optical flare onset are measured. In first approach it is assumed that the spectra are constant in shape during one event, that is, they differ only by a factor at different times.

August 22, 1958 event: The event of August 22, 1958[9] belongs to the five major events of the year 1958, some of the remaining were of higher intensity and duration. The riometer in College, Alaska (65° magnetic latitude) measured cosmic noise absorption of >10 db at 28 Mc.

[8]See also reference 7 for spectra and sources.

[9]See reference 48 for original data.

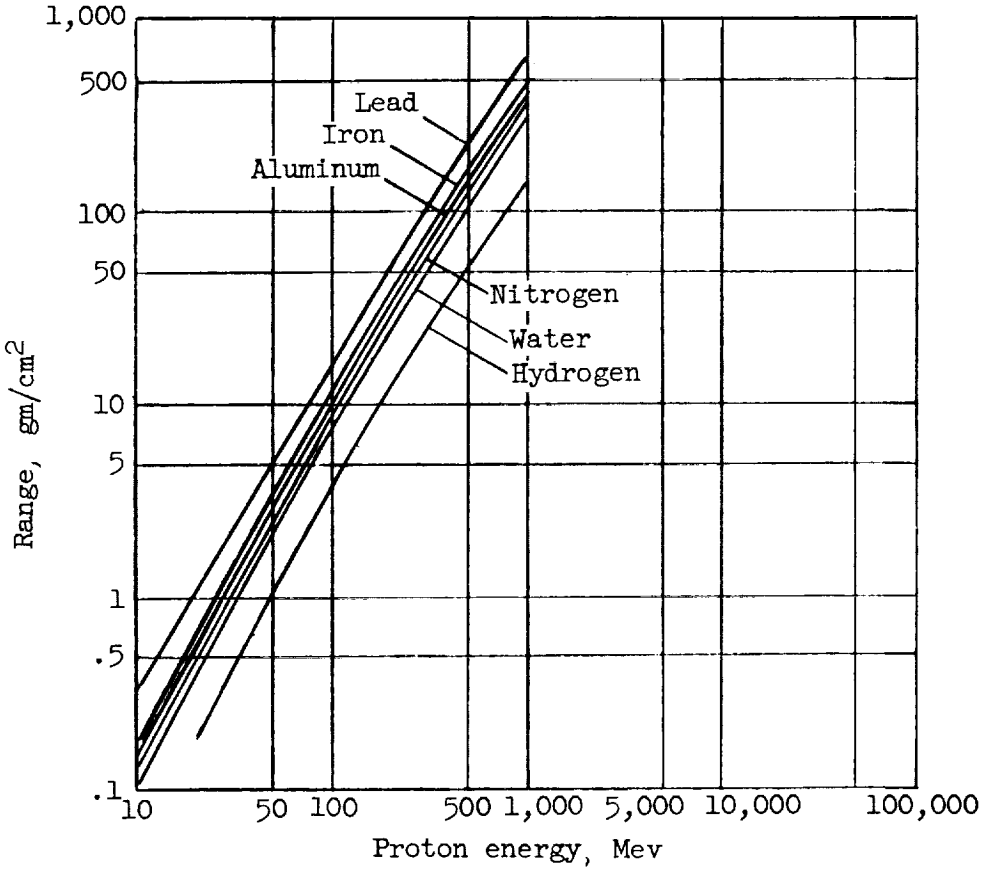

Figure 16.- Range of protons in different materials as function of the proton's kinetic energy.

The time profile of intensity of particles $E \gtrsim 100$ Mev in the maximum phase was measured in balloon flight 869 above Fort Churchill (83° magnetic latitude). Fourteen hours after the flare the spectrum $E > 100$ Mev was measured in balloon ascent 870 as $N(>E) = 10^9 E^{-4}$ particles/cm^2-sec (E in Mev). This spectrum was extrapolated down to 40 Mev and used as basis for the calculation of the dose rates at this particular instant. By following the intensity record over the time and using the dose rates $\dot{D}_{14}(x)$ calculated from the spectrum after 14 hours as point of reference, the lower limit of doses in figure 13 is obtained. An upper limit of doses is calculated by assuming for free space validity of the law $\dot{D} = D_o\left(\frac{t_o}{t}\right)^2$ suggested by Winckler and inserting $t_o = 2$ hours, again using $\dot{D}_{14}(x)$ as a reference. Dose values twice as high are obtained. The dose value behind few gram/cm^2 H_2O is smaller than 4 rep and falls off steeply with shield thickness x; thus, the shielding problem in this case is of lower magnitude.

May 10, 1959 event: The lower limit of doses for the frequently cited May 10, 1959 event[10] is calculated by assuming that the flux from the beginning of the proton surge as measured with the riometer in College, Alaska (65° magnetic latitude) remained constant at the peak value obtained with balloon above Minneapolis (55° magnetic latitude) after 33 hours when these particles reached this low latitude during magnetic disturbances, and then to fall off according to the presented riometer record.[11] The riometer of 28 Mc of Reid and Leinbach (ref. 40) in College, recording the time profile of intensity of low-energy particles, went off scale for 18 hours during the period of maximum flux. On the basis of an extrapolation of this riometer record which is however highly arbitrary, a five time higher upper limit of doses is given in figure 13.

July 14, 1959 event: In the case of the July 14, 1959 extreme intense event - apparently of shorter duration than the May event - the prompt dose rate for free space of 3×10^4 rep/hr of protons >40 Mev for the time 1 hour after the flare inferred by Winckler from comparison of balloon and Pioneer V measurements (the latter in a distance of 5×10^6 km from the earth) leads to values of total dose of the same order of magnitude as the above upper limit of the May event. For the dose calculation in the case of the July 14 event, a rapid increase of intensity in the first hour after the flare and then a decrease according to an inverse t^2 law and as reference point the flux after 31 hours and the same spectrum

---

[10] See reference 40 for riometer data and spectrum.

[11] A similar assumption and a similar calculation for carbon as shielding material was already made by W. Keller and N. M. Schaeffer (refs. 4 and 21) with substantially the same result. Essentially the same dose values are also reported by Fichtel (ref. 49) and Naugle (ref. 50) for a typical extreme flux low-energy event.

as that of May 10 is assumed. It is dubious, as emphasized by Winckler, that the rise time was only of the order of 1 to 2 hours and that the t^2 law is valid so close back to the time of the optical flare. These upper doses for extreme low-energy events should therefore be considered as highly conservative. An evaluation of more recently available riometer and ionospheric scattering data obtained during extreme-flux low-energy events may lead to substantially lower upper limits of doses in these events. On the other side the possibility remains that, even at polar latitudes near the earth, a part of the flux may be missed because distortions of the geomagnetic field or interplanetary fields may prevent particles from coming close to the earth. On some occasions the particles may have full access to a spacecraft outside the earth's magnetic field during the maximum intensity phases, undisturbed or even guided by interplanetary magnetic tongs originating on the sun according to the hypotheses of Gold, Carmichael, and other scientists.

The February 23, 1956 high-energy event.- In the case of this most intense high-energy event (observed since 1938) where particles with energies >20 Bev are found, two spectra are derived from the measurements: The prompt spectrum (Simpson, Van Allen, Winckler, refs. 51 to 53 and 6) and the 19-hour spectrum (Bailey, ref. 9). The spectra have different shape. The flux of high-energy particles (E > 1 Bev) decreased apparently much more rapidly with time (by a factor 4,000) than the flux in the low-energy part of the spectra (a factor of 20) during the considered 19 hours. The lower limit of doses in figure 13 was found by assuming that the prompt spectrum decreases as fast as the high-energy part according to an inverse t^2 law (really the decrease is about exponential, that is slower); thus dose values which are certainly too low are obtained. An upper limit of doses can be calculated by assuming that the prompt spectrum decreases with equal shape as slowly as the low-energy part according to an exponential time law. The upper limit given in figure 13 for the February 1956 event is by a factor 1.5 to 2 lower, when the fact that the influx of low-energy particles is generally delayed is taken into account. This upper limit is obtained by starting with the prompt dose-rate curve and by using the time decay law $\dot{D} = D_o\left(\frac{t_o}{t}\right)^2$ with energy-dependent t_o to fit the dose-rate curve after 19 hours. This assumption includes that the maximum of the low-energy flux in the hundredth of Mev range is delayed by about 3 hours. It may be mentioned that the flux values in the high-energy range of the prompt spectrum estimated by Winckler and adopted in these dose calculations are higher by a factor 5 to 10 than those estimated by other authors. (See refs. 51 and 38.) The above upper limit of doses appears therefore as a conservative estimate.

The November 12, 1960 medium-energy event.- The notation medium-energy event is used because the neutron intensity at sea level was increased only in high latitudes and because this increase was only in

the order of 100 percent above galactic cosmic-ray background and indicated low flux in the Bev range. On the other side, the intensity of low-energy particles in the hundredth of Mev range was very high. In the February 1956 high-energy event, the maximum of the neutron surge was 3,600 percent in high latitudes as seen in figure 11; a low increase of neutrons in mountain altitudes was observed even at the equator and pointed to a noticeable flux in the energy range above 14 Bev.

The lower limit of doses of the November 12, 1960 event (see fig. 13) is calculated by assuming that the spectra measured in photoemulsions (Fichtel and Guss) and scintillation counters (Davis and Ogilvie) in rockets 1840 UT (Nov. 12) and 1603 UT (Nov. 13) are valid for the 9 hours from 1430 to 2330 (Nov. 12) and 24.5 hours from 2330 (Nov. 12) to 2400 (Nov. 13), respectively. (See fig. 17.) The above spectrum 1840 (Nov. 12) is the spectrum at the intermediate minimum of the neutron surge (see fig. 17) 5 hours after the optical flare 3+ (Onset 1322, Nov. 12). The 1603 (Nov. 13) spectrum is measured 27 hours after the flare, nearly at the end of the event. (These lower limits of spectra are indicated in fig. 17; they lie in the 100 Mev range about 40 percent lower than the first and last of the three spectra given in fig. 9, that are derived from a greater amount of data.) Thus the time-integrated fluxes and doses based on these spectra during the given time periods are considered as lower limits. (See fig. 13, lower limit of doses.)

To estimate upper limits of fluxes and doses in this event, the spectra indicated in figures 9 and 17 are used. These spectra are composed in the following way: During the maximum period of the neutron flux in Deep River (1430 to 2330, November 12), the flux in the high-energy range must have been higher than at the minimum 1840. Therefore, an average spectrum for the period 1430 to 2330, November 12, is given in figures 9 and 17 which uses in the low-energy range the scintillation measurements of Davis and Ogilvie at 1840 and in the medium- and high-energy range the emulsion measurements of Fichtel and Guss, the latter multiplied by a suitable factor to meet with a slope E^{-3} the point at 2 Bev estimated by Van Allen for this period on the basis of the neutron data.

For the instant 2330 and 4 hours later, Van Allen's estimate at 2 Bev and his measurement $N(E > 30$ Mev) with Explorer VII, the one point of the Fichtel and Guss measurements at 150 Mev with the rocket at 2330, and in the low-energy range the values of Davis and Ogilvie for 2330, November 12, are used.

As upper spectrum in the last period 330 to 2130, November 13, the values of Davis and Ogilvie at 1603 in the low-energy range ($E < 50$ Mev) and the spectrum measured by Winckler in balloon ascent at 2122, November 13, in the high-energy range ($E > 100$ Mev) were used. Winckler's spectrum is extrapolated back to the time 1603 by means of his time profile of intensity $E > 100$ Mev (ref. 8).

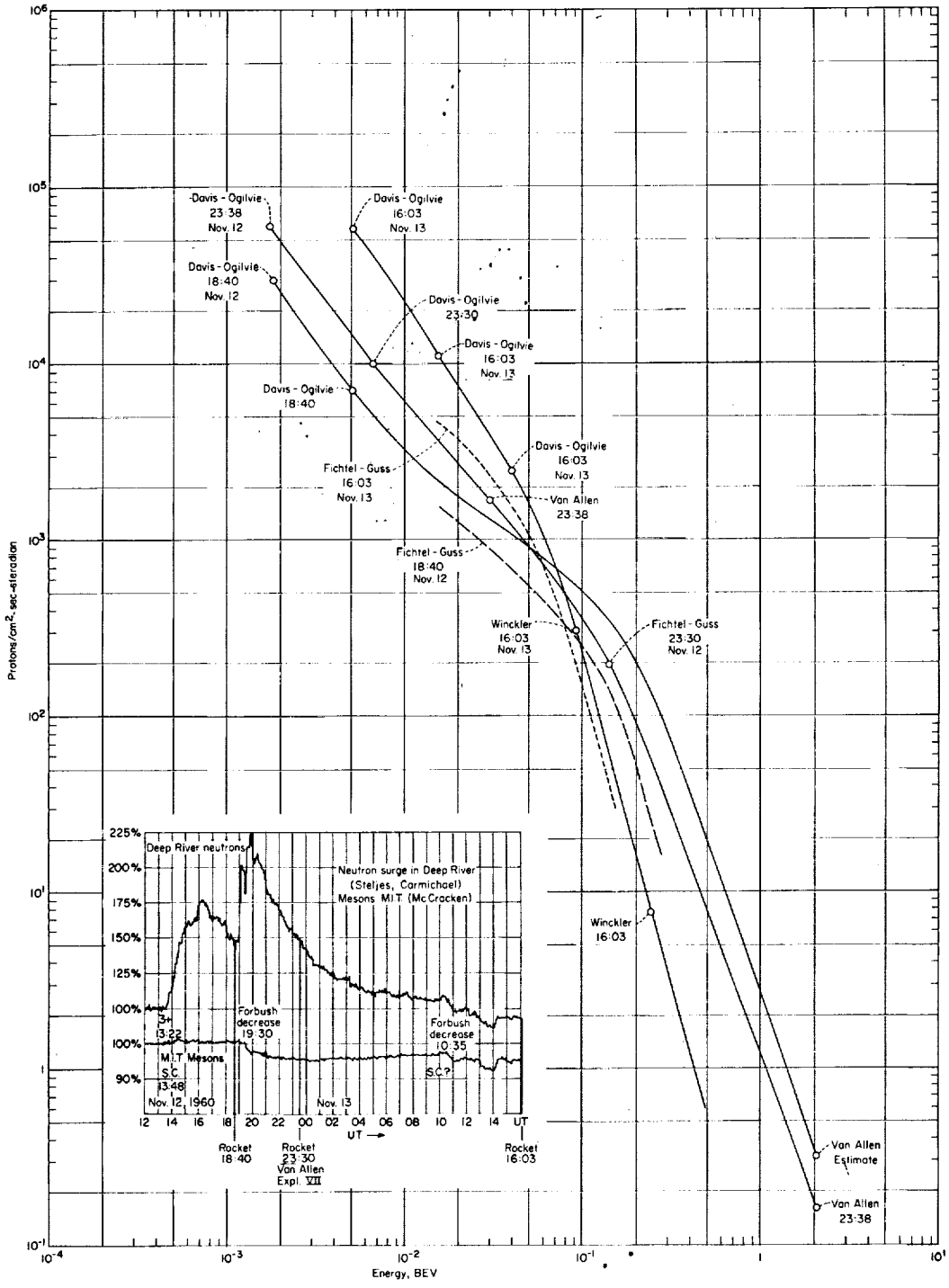

Figure 17.- Spectra of the November 12, 1960 event from which the upper and lower limits of doses given in figure 13 are derived.

The flux values of Davis and Ogilvie at 1603 in the low-energy range are higher than those of Fichtel and Guss within the same rocket shot. The values in the medium-energy range (90 to 350 Mev) at 1603 extrapolated from Winckler's balloon measurements at 2122 and his intensity time profile are found also to be about 60 percent higher than the emulsion measurements of Fichtel and Guss at 1603. The former values are therefore considered as upper limits of fluxes at 1603.

By integrating the fluxes given by these spectra over the corresponding time periods, the following upper and lower limits of time-integrated fluxes in protons/cm^2 are obtained.

November 12, 1960

Energy	E > 40 Mev	E > 80 Mev	E > 100 Mev	E > 200 Mev
protons/cm^2	2×10^9 to 3×10^9	4.8×10^8 to 7.3×10^8	2.6×10^8 to 4.5×10^8	2.2×10^7 to 9.6×10^7

In this calculation the assumption is made that the particles arrive isotropic from the onset. Within the first 9 hours, a period when isotropy is part of the time in doubt, the flux >40 Mev does not surpass 3 to 4.5×10^8 protons/cm^2; hence, the numbers for the total flux >40 Mev are not substantially affected by this simplifying assumption.

The lower limit of the time-integrated flux E > 40 Mev for this event is by about a factor 1.5 to 2 higher than Van Allen's result, 2×10^9 protons/cm^2 for the November 12 and 15 event, since both events were of comparable size. The dose value behind 2 g/cm^2, for November 12, of 600 to 800 rep is roughly in agreement with the value 700r given by Van Allen for both events in the meeting of the NASA Energetic Particle and Field Subcommittee in Boulder, Colorado, on October 5, 1961.

REFERENCES

1. Van Allen, James A., and Frank, Louis A.: Radiation Around the Earth to a Radial Distance of 107,000 km. Nature, vol. 183, no. 4659, Feb. 14, 1959, pp. 430-434.

2. Freden, Stanley C., and White, R. Stephen: Protons in the Earth Magnetic Field. Phys. Rev. Letters, vol. 3, no. 1, July 1, 1959, pp. 9-10.

3. Schaefer, Hermann J.: Tissue Depth Doses in the High Intensity Proton Radiation Field of the Inner Van Allen Belt. Rep. No. 16, U.S. Naval School of Aviation Medicine (Pensacola, Fla.), Nov. 10, 1959.

4. Keller, J. W., and Schaeffer, N. M.: Shielding of Manned Vehicles From Space Radiation. Paper presented at 31st Annual Meeting of Aero-Space Medical Assoc. (Miami Beach, Fla.), May 1960.

5. Allen, R. I., Dessler, A. J., Perkins, J. F., and Price, H. C.: Shielding Problems in Manned Space Vehicles. NR-104 (Contract No. DA-01-009-506-ORD-832), Lockheed Nuclear Products (Marietta, Ga.), July 1960.

6. Winckler, J. R.: Primary Cosmic Rays. Proceedings of Conference on Radiation Problems in Manned Space Flight. George J. Jacobs, ed., NASA TN D-588, 1960, pp. 72-93. (Also published in Radiation Res., vol. 14, no. 5, May 1961, pp. 521-539.)

7. Foelsche, Trutz: Protection Against Solar Flare Protons. (Presented at Seventh Annual Meeting of American Astronautical Society, Dallas, Texas, Jan. 16-18, 1961.) Preprint 61-34, Amer. Astronautical Soc., Jan. 1961.

8. Winckler, J. R.: Solar Influences on the Radiation Field in Space. Paper presented at 32nd Annual Meeting, Aerospace Medical Association (Chicago), Apr. 25, 1961.

9. Bailey, D. K.: Abnormal Ionization in the Lower Ionosphere Associated With Cosmic-Ray Flux Enhancements. Proc. Inst. Radio Engineers, vol. 47, no. 2, Feb. 1959, pp. 255-266.

10. Van Allen, James A.: The Geomagnetically Trapped Corpuscular Radiation. Jour. Geophys. Res., vol. 64, no. 11, Nov. 1959, pp. 1683-1689.

11. Van Allen, James A., and Frank, Louis A.: Radiation Measurements to 658,300 km With Pioneer IV. Nature, vol. 184, no. 4682, July 25, 1959, pp. 219-224.

12. Arnoldy, R. L., Hoffman, R. A., and Winckler, J. R.: Observations of Van Allen Radiation Regions During Geomagnetic Storms. Observations of Corpuscular Radiation With Satellites and Space Probes. IGY Satellite Rep. No. 11, Nat. Acad. Sci., June 1960, pp. 89-104.

13. Naugle, John E., and Kniffen, Donald A.: The Flux and Energy Spectra of the Protons in the Inner Van Allen Belt. NASA TN D-412, 1961.

14. Pizzella, Guido, McIlwain, C. E., and Van Allen, J. A.: Time Variations of Intensity in the Earth's Inner Radiation Zone, October 1959 through December 1960. Jour. Geophys. Res., vol. 67, no. 4, Apr. 1962, pp. 1235-1253.

15. O'Brien, B. J., Van Allen, J. A., Laughlin, C. D., and Frank, L. A.: Absolute Electron Intensities in the Heart of the Earth's Outer Radiation Zone. Jour. Geophys. Res. (Letters to the Editor), vol. 67, no. 1, Jan. 1962, pp. 397-403.

16. Hoffman, R. A., Arnoldy, R. L., and Winckler, J. R.: Observations of the Van Allen Radiation Regions During August and September 1959. 3. The Inner Belt. Jour. Geophys. Res., vol. 67, no. 1, Jan. 1962, pp. 1-12.

17. Vernov, S. N., and Chudakov, A. E.: Terrestrial Corpuscular Radiation and Cosmic Rays. Space Research, Hilde Kallmann Bijl, ed., North Holland Publ. Co. (Amsterdam), 1960, pp. 910-920.

18. Vernov, S. N., Chudakov, A. E., Vakulov, P. V., Logashev, Yu. I., and Nikolayev, A. G.: Radiation Measurements During the Flight of the Second Soviet Space Rocket. Space Research, Hilde Kallmann Bijl, ed., North Holland Publ. Co. (Amsterdam), 1960, pp. 845-851.

19. Heckman, Harry H., and Armstrong, Alice H.: Energy Spectrum of Geomagnetically Trapped Protons. Jour. Geophys. Res., vol. 67, no. 4, Apr. 1962, pp. 1255-1262.

20. Smith, R. V., Fisher, P. C., Imhof, W. L., and Reagan, J. B.: Midas IV Proton Measurement in the Inner Van Allen Belt. [Rep.] 3-77-62-6 (Contract AF 19(604)-8028) Nuclear Phys. Dept., Lockheed Missiles and Space Corp., Feb. 1962.

21. Keller, J. W.: A Study of Shielding Requirements for Manned Space Missions. FZK-124 (Contract No. NASw-50), Convair, Oct. 10, 1960.

22. Holly, Frances E., and Johnson, Richard G.: Measurement of Radiation in the Lower Van Allen Belt. Jour. Geophys. Res., vol. 65, no. 2, Feb. 1960, pp. 771-772.

23. Walt, M. W., Chase, L. F., Jr., Cladis, J. B., Imhof, W. L., and Knecht, D. J.: Energy Spectra and Altitude Dependence of Electrons Trapped in the Earth's Magnetic Field. Space Research, Hilde Kallmann Bijl, ed., North Holland Publ. Co. (Amsterdam), 1960, pp. 910-920.

24. Dye, D. L., and Noyes, J. C.: Biological Shielding for Radiation Belt Particles. Jour. Astronautical Sci., vol. VII, no. 3, Fall 1960, pp. 64-70.

25. Evans, Robley D.: Principles for the Calculation of Radiation Dose Rates in Space Vehicles. Report 63270-05-01 (Contract NAS 5-664), Arthur D. Little, Inc. (Cambridge, Mass.), July 1961.

26. Fan, C. Y., Meyer, Peter, and Simpson, J. A.: Rapid Reduction of Cosmic-Radiation Intensity Measured in Interplanetary Space. Phys. Rev. Letters, vol. 5, no. 6, Sept. 15, 1960, pp. 269-271.

27. Schaefer, Hermann J.: Definition of a Permissible Dose for Primary Cosmic Radiation. Jour. Aviation Medicine, vol. 25, no. 4, Aug. 1954, pp. 392-398.

28. Wallner, Lewis E., and Kaufman, Harold R.: Radiation Shielding for Manned Space Flight. NASA TN D-681, 1961.

29. Anon.: Background Material for the Development of Radiation Protection Standards. Rep. No. 1, Federal Radiation Council, May 13, 1960.

30. Schaefer, Hermann J.: Exposure Hazards From Cosmic Radiation Beyond the Stratosphere and in Free Space. Jour. Aviation Medicine, vol. 23, no. 4, Aug. 1952, pp. 334-344.

31. Simons, David G.: Manhigh II. AFMDC-TR-59-28, ASTIA Doc. No. AD-216892, U.S. Air Force, June 1959.

32. Yagoda, Herman: Cosmic-Ray Monitoring of the Manned Stratolab Balloon Flights. Geophys. Res. Directoriate Res. Note No. 43 (AFCRL-TN-60-640), Air Force Cambridge Res. Labs., Sept. 1960.

33. Anderson, Kinsey A.: Preliminary Study of Prediction Aspects of Solar Cosmic-Ray Events. NASA TN D-700, 1961.

34. Reid, George C., and Leinbach, Harold: Low-Energy Cosmic-Ray Events Associated With Solar Flares. Jour. Geophys. Res., vol. 64, no. 11, Nov. 1959, pp. 1801-1805.

35. Adamson, David, and Davidson, Robert E.: Statistics of Solar Cosmic Rays as Inferred From Correlation With Intense Geomagnetic Storms. NASA TN D-1010, 1962.

36. Ney, E. P., and Stein, W.: Solar Cosmic Rays in November 1960. Jour. Geophys. Res. (Abstracts), vol. 66, no. 8, Aug. 1961, p. 2,550.

37. Schaefer, H. J.: Further Evaluation of Tissue Depth Doses in Proton Radiation Fields in Space. Rep. No. 17, U.S. Naval School of Aviation Medicine (Pensacola, Fla.), May 24, 1960.

38. Schaefer, Hermann J.: Radiation and Man in Space. Advances in Space Science, vol. 1, Academic Press, Inc. (New York), 1959, pp. 267-339.

39. Steljes, J. F., Carmichael, H., and McCracken, K. G.: Characteristics and Fine Structure of the Large Cosmic-Ray Fluctuations in November 1960. Jour. Geophys. Res., vol. 66, no. 5, May 1961, pp. 1363-1377.

40. Reid, G. C., and Leinbach, H.: Morphology and Interpretation of the Great Polar Cap Absorption Events of May and July 1959. Geophysical Institute, Univ. of Alaska (College, Alaska), Apr. 1, 1960.

41. Ogilvie, K. W., Bryant, D. A., and Davis, L. R.: Rocket Observations of Solar Protons During the November 12, 1960 Event. Goddard Space Flight Center Contributions to 1961 Kyoto Conference on Cosmic Rays and the Earth Storm. NASA TN D-1061, 1962, pp. 47-54.

42. Fichtel, C. E., and Guss, D. E.: Heavy Nuclei in Solar Cosmic Rays. Goddard Space Flight Center Contributions to 1961 Kyoto Conference on Cosmic Rays and the Earth Storm. NASA TN D-1061, 1962, pp. 55-62.

43. Allen, R. I., Bly, F. T., Dessler, A. J. Douglass, C. C., Perkins, J. F., Price, H. C., Schofield, W. M., and Smith, E. C. (J. H. Tolan, ed.): Annual Report - 1960: Shielding Problems in Manned Space Vehicles. NR-140 (Contract No. DA-01-009-506-ORD-832), Lockheed Nuclear Products (Marietta, Ga.), Sept. 1961.

44. Weinberg, Alvin M.: Impact of Large-Scale Science on the United States. Science, vol. 134, no. 3473, July 21, 1961, pp. 161-164.

45. Aron, W. A., Hoffman, B. G., and Williams, F. C.: Range-Energy Curves. AECU-663, U.S. Atomic Energy Commission, May 28, 1951.

46. Rich, Marvin, and Madey, Richard: Range Energy Tables. UCRL-2301 (Contract No. W-7405-eng-48), Radiation Lab., Univ. of California, Mar. 1954. (Available from OTS, Dept. Commerce.)

47. Rossi, Bruno: High-Energy Particles. Prentice Hall, Inc., 1956.

48. Anderson, K. A., Arnoldy, R., Hoffman, R., Peterson, L., and Winckler, J. R.: Observations of Low-Energy Solar Cosmic Rays From the Flare of 22 August 1958. Jour. Geophys. Res., vol. 64, no. 9, Sept. 1959, pp. 1133-1147.

49. Anderson, Kinsey A., and Fichtel, Carl E.: Discussions of Solar Proton Events and Manned Space Flight. NASA TN D-671, 1961.

50. Naugle, John E.: Space Radiation Levels. Nucleonics, vol. 19, no. 4, Apr. 1961, pp. 89-91.

51. Meyer, P., Parker, E. N., and Simpson, J. A.: Solar Cosmic Rays of February 1956, and Their Propagation Through Interplanetary Space. Phys. Rev., vol. 104, no. 3, second ser., Nov. 1, 1956, pp. 768-783.

52. Winckler, John R.: Cosmic-Ray Increase at High Altitude on February 23, 1956. Phys. Rev., vol. 104, no. 1, second ser., Oct. 1, 1956, p. 220.

53. Van Allen, J. A., and Winckler, J. R.: Spectrum of Low-Rigidity Cosmic Rays During the Solar Flare of February 23, 1956. Phys. Rev., vol. 106, no. 5, June 1, 1957, pp. 1072-1073.

NASA-Langley, 1962 L-1962

NASA TN D-1267
National Aeronautics and Space Administration.
CURRENT ESTIMATES OF RADIATION DOSES IN SPACE. Trutz Foelsche. July 1962. 51p. OTS price, $1.25. (NASA TECHNICAL NOTE D-1267)

A gross survey of data on energetic radiation in the environment of the earth is presented. This survey embraces the Van Allen belt radiations, galactic cosmic radiations, and solar cosmic radiations associated with solar flares. In the light of the current data the radiation problem is analyzed in terms of shielding requirements to keep exposure down to "tolerable" limits in manned space flights. The estimates are preliminary especially in the cases of chance encounter with flare protons, since the available data are incomplete and only allow calculations of upper and lower limits of physical doses. Also the contribution of certain primaries and secondaries to the biological effect is not finally known.

I. Foelsche, Trutz
II. NASA TN D-1267

(Initial NASA distribution:
2, Aerodynamics, missiles and space vehicles;
7, Astrophysics;
8, Behavioral studies;
9, Biomedicine;
26, Materials, other;
31, Physics, nuclear and particle; 47, Satellites;
48, Space vehicles;
52, Structures;
53, Vehicle performance.)

NASA

NASA TN D-1267
National Aeronautics and Space Administration.
CURRENT ESTIMATES OF RADIATION DOSES IN SPACE. Trutz Foelsche. July 1962. 51p. OTS price, $1.25. (NASA TECHNICAL NOTE D-1267)

A gross survey of data on energetic radiation in the environment of the earth is presented. This survey embraces the Van Allen belt radiations, galactic cosmic radiations, and solar cosmic radiations associated with solar flares. In the light of the current data the radiation problem is analyzed in terms of shielding requirements to keep exposure down to "tolerable" limits in manned space flights. The estimates are preliminary especially in the cases of chance encounter with flare protons, since the available data are incomplete and only allow calculations of upper and lower limits of physical doses. Also the contribution of certain primaries and secondaries to the biological effect is not finally known.

I. Foelsche, Trutz
II. NASA TN D-1267

(Initial NASA distribution:
2, Aerodynamics, missiles and space vehicles;
7, Astrophysics;
8, Behavioral studies;
9, Biomedicine;
26, Materials, other;
31, Physics, nuclear and particle; 47, Satellites;
48, Space vehicles;
52, Structures;
53, Vehicle performance.)

NASA

NASA TN D-1267
National Aeronautics and Space Administration.
CURRENT ESTIMATES OF RADIATION DOSES IN SPACE. Trutz Foelsche. July 1962. 51p. OTS price, $1.25. (NASA TECHNICAL NOTE D-1267)

A gross survey of data on energetic radiation in the environment of the earth is presented. This survey embraces the Van Allen belt radiations, galactic cosmic radiations, and solar cosmic radiations associated with solar flares. In the light of the current data the radiation problem is analyzed in terms of shielding requirements to keep exposure down to "tolerable" limits in manned space flights. The estimates are preliminary especially in the cases of chance encounter with flare protons, since the available data are incomplete and only allow calculations of upper and lower limits of physical doses. Also the contribution of certain primaries and secondaries to the biological effect is not finally known.

I. Foelsche, Trutz
II. NASA TN D-1267

(Initial NASA distribution:
2, Aerodynamics, missiles and space vehicles;
7, Astrophysics;
8, Behavioral studies;
9, Biomedicine;
26, Materials, other;
31, Physics, nuclear and particle; 47, Satellites;
48, Space vehicles;
52, Structures;
53, Vehicle performance.)

NASA

NASA TN D-1267
National Aeronautics and Space Administration.
CURRENT ESTIMATES OF RADIATION DOSES IN SPACE. Trutz Foelsche. July 1962. 51p. OTS price, $1.25. (NASA TECHNICAL NOTE D-1267)

A gross survey of data on energetic radiation in the environment of the earth is presented. This survey embraces the Van Allen belt radiations, galactic cosmic radiations, and solar cosmic radiations associated with solar flares. In the light of the current data the radiation problem is analyzed in terms of shielding requirements to keep exposure down to "tolerable" limits in manned space flights. The estimates are preliminary especially in the cases of chance encounter with flare protons, since the available data are incomplete and only allow calculations of upper and lower limits of physical doses. Also the contribution of certain primaries and secondaries to the biological effect is not finally known.

I. Foelsche, Trutz
II. NASA TN D-1267

(Initial NASA distribution:
2, Aerodynamics, missiles and space vehicles;
7, Astrophysics;
8, Behavioral studies;
9, Biomedicine;
26, Materials, other;
31, Physics, nuclear and particle; 47, Satellites;
48, Space vehicles;
52, Structures;
53, Vehicle performance.)

NASA